People's Democratic Republic of Algeria

Ministry of Higher Education and Scientific Research

University of Ghardaïa

Faculty of Science and Technology

Department of Mathematics and Computer Science

MASTER'S THESIS

Submitted in partial fulfillment of the requirements for the Master's Degree

In **Computer Science**

Specialization: Intelligent Systems for Knowledge Extraction (SIEC)

Presented by: Bega Ahlam & Adjila Amina

Thesis Title

CT Dose Optimization and Personalized Radiation Risk Assessment for Pediatric Patients using AI

Jury members

Dr. Slimane Bellaouar	MCA	Univ. Ghardaïa	Président
M. Abdelfateh Bekkair	MAB	Univ. Ghardaïa	Examinateur
M. Saad Boudabia	MCA	Univ. Ghardaia	Supervisor
M. Youcef Mahdjoub	MAA.	Univ. Ghardaïa	Co-Supervisor

Academic Year 2025/2026

Acknowledgements

First and foremost, we thank God Almighty with praise and gratitude for His blessings and grace, which enabled us to complete this work . Nothing is achieved except by His will and support.

We extend our deepest appreciation and heartfelt thanks to our parents for their unconditional love, continuous support, great sacrifices, and prayers, which have been our strongest source of strength throughout this journey.

We are profoundly grateful to our supervisors, Prof Boudabia Saad and Prof Mahjoub Youssef, for their valuable advice and insightful guidance throughout the development of this work.

We also express our sincere thanks and respect to the members of the examination committee for agreeing to evaluate and review our work.

Finally, we would like to thank everyone who supported us, whether directly or indirectly, through encouragement, assistance, or motivation. To all of you, we offer our deepest gratitude and appreciation.

Dedication

To my beloved Mother and dear Father
From the moment I was born until today, you have been my light, my strength, and my safe haven. I dedicate this work to you for your support, sacrifices, and unconditional love. You are the greatest blessing in my life. May Allah reward you abundantly.

To my sisters Meriem, Hadjar, and Asma:
Thank you for your love, patience, and believe in me. I am truly blessed to have you.

To my beloved grandmother Maaziza (may Allah have mercy on her)
Though you are no longer with us, your love and memory remain in my heart. This achievement is for your beautiful soul.

To all my family, young and old:
Thank you for your love, support, and prayers.

To my notebook companion and best friend Ahlam, and my dear friends Afrah, Darine, Dalal, and all my university friends
Thank you for the memories, support, and unforgettable friendship.

Adjila Amina

Dedication

To my beloved Mother and dear Father,

Your love has been the foundation upon which I built my dreams, and your guidance has illuminated every step of my journey. Throughout my life, you have given me far more than I could ever repay: your time, your sacrifices, your patience, and your unwavering faith in me.

Whenever I faced difficulties, your encouragement gave me strength, your belief in me gave me confidence. This achievement is not mine alone; it is the result of your endless support and the values you instilled in me.

Words cannot fully express the depth of my gratitude and love for you. May Allah bless you with good health, happiness, and a long life filled with peace and joy. I will always be proud to be your daughter.

To my entire family, from the eldest to the youngest, thank you for your love, support, encouragement, and prayers. Your presence in my life has been a constante source of strength and motivation, and I am deeply grateful to each and every one of you.

To my notebook companion and best friend Amina, thank you for your friendship, support, and the beautiful moments we shared throughout this journey.

To my dearest friends Meriem, Afrah, and Dalal, who stood by my side and supported me throughout my university years, thank you for your encouragement, kindness, and unforgettable friendship.

Bega Ahlam

الملخص

يعد التصوير المقطعي المحوسب (CT) من أكثر الفحوصات الإشعاعية شيوعاً، إلا أن تخصيص جرعاته لدى الأطفال يمثل تحدياً بالغاً، نظراً لحساسيتهم الإشعاعية العالية وافتقار الأساليب التقليدية إلى التخصيص الفردي. لذا، تهدف هذه الدراسة إلى بناء إطار عمل قائم على التعلم الآلي لإنجاز ثلاث مهام أساسية :الانحدار (Regression) للتنبؤ بقيم مؤشري الجرعة CTDIvol وDLP، والتصنيف (Classification) لتقسيم المرضى إلى ثلاث فئات من المخاطر الإشعاعية (منخفضة، متوسطة، مرتفعة)، والتوصية (Recommendation)باقتراح بروتوكولات تصوير مناسبة لكل مريض، وذلك بما يتوافق مع مبدأ ALARA الهادف إلى تقليل التعرض للإشعاع إلى أدنى مستوى ممكن دون التأثير على الجودة التشخيصية.

اعتمدت المنهجية على بيانات 359 مريضاً من الأطفال، وشملت متغيرات سريرية (العمر، الوزن، قطر الجسم) وتقنية(kVp ، mAs)، وتمت مقارنة أربعة نماذج للتعلم الآلي: الغابة العشوائية (Random Forest) ، والتعزيز التدريجي(Gradient Boosting) ، وآلة المتجهات الداعمة(SVM) ، والإدراك متعدد الطبقات .(MLP) أظهرت النتائج تفوق نموذج Gradient Boostingفي مهام الانحدار، حيث حقق معامل تحديد (R^2) بلغ 0.9825 للتنبؤ بـ CTDIvol و0.9424 للتنبؤ بـDLP ، في حين تفوق نموذج MLPفي تصنيف المخاطر الإشعاعية بدقة 87.5% ودرجة F1-score بلغت 0.8723. كما أكد تحليل أهمية المتغيرات أن العوامل التقنية خاصة (mAs) وقطر الجسم هي المحددات الأكثر تأثيراً على الجرعة، مما يوفر أساساً قوياً لأنظمة دعم القرار السريري القائمة على التوصية الشخصية. ومع ذلك، تشير الدراسة إلى محدودية حجم العينة واقتصار البيانات على أجهزة GEوSiemens، مما يستدعي توسيع قاعدة البيانات مستقبلاً وتعزيزها بمقاييس موضوعية لجودة الصورة، لتعزيز دقة التصنيف والتوصية.

الكلمات المفتاحية :التصوير المقطعي المحوسب(CT) ، تحسين الجرعة الإشعاعية، التعلم الآلي، التنبؤ بالجرعة، تصنيف المخاطر الإشعاعية، طب الأطفال، مبدأALARA ، دعم القرار السريري.

Abstract

Computed Tomography (CT) is one of the most commonly used radiological examinations; however, dose optimization in pediatric patients poses a significant challenge due to their higher radiosensitivity and the lack of individualized approaches in conventional methods. Therefore, this study aims to develop a machine learning-based framework to accomplish three core tasks: Regression to predict CTDIvol and DLP dose indices, Classification to stratify patients into three radiation risk categories (low, moderate, high), and Recommendation to suggest appropriate imaging protocols based on each patient's characteristics, all in compliance with the ALARA principle (As Low As Reasonably Achievable), which seeks to minimize radiation exposure to the lowest possible level without compromising diagnostic image quality.

The methodology was applied to a dataset of 359 pediatric patients, incorporating clinical variables (age, weight, body diameter) and technical parameters (mAs, kVp). Four machine learning models were compared: Random Forest, Gradient Boosting, Support Vector Machine (SVM), and Multilayer Perceptron (MLP). The results demonstrated that the Gradient Boosting model outperformed others in regression tasks, achieving an R^2 of 0.9825 for CTDIvol prediction and 0.9424 for DLP prediction. Meanwhile, the MLP model achieved the best performance in radiation risk classification, with an accuracy of 87.5% and an F1-score of 0.8723. Feature importance analysis further confirmed that technical factors (particularly mAs) and body diameter are the most influential determinants of radiation dose, providing a robust foundation for clinical decision support systems based on personalized recommendations.

Nevertheless, the study acknowledges certain limitations, including the relatively small sample size and the restriction of data to GE and Siemens scanners, which underscores the need for future expansion of the database and the integration of objective image quality metrics to enhance the accuracy of classification and recommendation tasks.

Keywords: Computed Tomography (CT), Radiation Dose Optimization, Machine Learning, Dose Prediction, Radiation Risk Classification, Pediatrics, ALARA Principle, Clinical Decision Support.

Résumé

La tomodensitométrie (TDM) est l'un des examens radiologiques les plus couramment pratiqués ; cependant, l'optimisation des doses chez les enfants représente un défi majeur, en raison de leur radiosensibilité accrue et de l'absence d'approches personnalisées dans les méthodes conventionnelles. Ainsi, cette étude vise à développer un cadre basé sur l'apprentissage automatique pour accomplir trois tâches fondamentales : la régression (Regression) pour prédire les indices de dose CTDIvol et DLP, la classification (Classification) pour répartir les patients en trois catégories de risque radiologique (faible, modéré, élevé), et la recommandation (Recommendation) pour proposer des protocoles d'imagerie adaptés à chaque patient, conformément au principe ALARA (As Low As Reasonably Achievable), qui vise à réduire l'exposition aux rayonnements au niveau le plus bas possible sans compromettre la qualité diagnostique.

La méthodologie a été appliquée à un ensemble de données portant sur 359 patients pédiatriques, incluant des variables cliniques (âge, poids, diamètre corporel) et des paramètres techniques (mAs, kVp). Quatre modèles d'apprentissage automatique ont été comparés : Forêt Aléatoire (Random Forest), Gradient Boosting, Machine à Vecteurs de Support (SVM), et Perceptron Multicouche (MLP). Les résultats ont montré que le modèle Gradient Boosting surpassait les autres dans les tâches de régression, avec un coefficient de détermination (R^2) de 0,9825 pour la prédiction du CTDIvol et de 0,9424 pour celle du DLP. En revanche, le modèle MLP a obtenu les meilleures performances en classification des risques radiologiques, avec une précision de 87,5 % et un score F1 de 0,8723. L'analyse de l'importance des variables a également confirmé que les facteurs techniques (notamment le mAs) et le diamètre corporel sont les déterminants les plus influents de la dose, offrant ainsi une base solide pour les systèmes d'aide à la décision clinique fondés sur des recommandations personnalisées.

Cependant, l'étude reconnaît certaines limites, notamment la taille restreinte de l'échantillon et la restriction des données aux appareils GE et Siemens, ce qui souligne la nécessité d'étendre à l'avenir la base de données et d'y intégrer des mesures objectives de qualité d'image, afin de renforcer la précision des tâches de classification et de recommandation.

Mots-clés : Tomodensitométrie (TDM), Optimisation de la Dose Radiologique, Apprentissage Automatique, Prédiction de Dose, Classification des Risques Radiologiques, Pédiatrie, Principe ALARA, Aide à la Décision Clinique.

Contents

List of Figures

List of Tables

List of Acronyms

CT : Computed Tomography (Tomodensitométrie ou scanner)
ALARA : As Low As Reasonably Achievable (Principe d'optimisation de la dose : aussi bas que raisonnablement possible)
CTDIvol : Volume Computed Tomography Dose Index (Indice de dose tomodensitométrique volumique)
DLP : Dose-Length Product (Produit dose-longueur)
MLP : Multi-Layer Perceptron (Perceptron multicouche)
SVM : Support Vector Machine (Machine à vecteurs de support)
RF : Random Forest (Forêt aléatoire)
GB : Gradient Boosting (Boosting par gradient)
ICRP : International Commission on Radiological Protection (Commission internationale de protection radiologique)
IAEA : International Atomic Energy Agency (Agence internationale de l'énergie atomique)
WHO : World Health Organization (Organisation mondiale de la santé)
AAPM : American Association of Physicists in Medicine (Association américaine des physiciens médicaux)
LNT : Linear No-Threshold (Modèle linéaire sans seuil)
DSB : Double-Strand Break (Cassure double-brin de l'ADN)
SSB : Single-Strand Break (Cassure simple-brin de l'ADN)
ROS : Reactive Oxygen Species (Espèces réactives de l'oxygène)
DDR : DNA Damage Response (Réponse aux dommages de l'ADN)
LET : Linear Energy Transfer (Transfert d'énergie linéique)
MRI : Magnetic Resonance Imaging (Imagerie par résonance magnétique)
BMI : Body Mass Index (Indice de masse corporelle)
TNM : Tumor, Node, Metastasis (Système de classification des tumeurs)
RECIST : Response Evaluation Criteria in Solid Tumors (Critères d'évaluation de la réponse dans les tumeurs solides)
CAD : Computer-Aided Diagnosis (Diagnostic assisté par ordinateur)
CNN : Convolutional Neural Network (Réseau de neurones convolutif)
DLR : Deep Learning Reconstruction (Reconstruction par apprentissage profond)
FBP : Filtered Back Projection (Rétroprojection filtrée)
MBIR : Model-Based Iterative Reconstruction (Reconstruction itérative basée sur un modèle)
GAN : Generative Adversarial Network (Réseau antagoniste génératif)
ANFIS : Adaptive Neuro-Fuzzy Inference System (Système d'inférence neuro-flou adaptatif)
XAI : Explainable Artificial Intelligence (Intelligence artificielle explicable)
AI : Artificial Intelligence (Intelligence artificielle)

ML : Machine Learning (Apprentissage automatique)
PCCT : Photon-Counting Computed Tomography (Tomodensitométrie à comptage de photons)
PCD : Photon-Counting Detector (Détecteur à comptage de photons)
EID : Energy-Integrating Detector (Détecteur intégrant l'énergie)
SNR : Signal-to-Noise Ratio (Rapport signal sur bruit)
CNR : Contrast-to-Noise Ratio (Rapport contraste sur bruit)
HIR : Hybrid Iterative Reconstruction (Reconstruction itérative hybride)
LDCT : Low-Dose Computed Tomography (Tomodensitométrie à faible dose)
TCIA : The Cancer Imaging Archive (Archive d'imagerie du cancer)
DICOM : Digital Imaging and Communications in Medicine (Imagerie numérique et communications en médecine)
kVp : Kilovoltage peak (Tension maximale en kilovolts)
mAs : Milliampere-second (Produit courant-temps en milliampère-seconde)
MAE : Mean Absolute Error (Erreur absolue moyenne)
RMSE : Root Mean Square Error (Erreur quadratique moyenne)
R^2 : Coefficient of determination (Coefficient de détermination)
SHAP : SHapley Additive exPlanations (Explications additives de Shapley)
LIME : Local Interpretable Model-agnostic Explanations (Explications locales interprétables indépendantes du modèle)
CDS : Clinical Decision Support (Soutien à la décision clinique)
LAR : Lifetime Attributable Risk (Risque attribuable à vie)

Introduction

Computed Tomography (CT) scans are widely used in modern medicine because they provide high-resolution images that are essential for diagnosing and treating a wide range of diseases. However, this powerful imaging modality also presents a significant challenge: the risk of exposing patients to ionizing radiation. Through personalized radiation risk assessment, each patient's risk can be estimated using multiple variables, including age, sex, weight, and prior exposure to radiation. Concurrently, CT dose optimization is an approach designed to minimize the radiation dose while preserving diagnostic image quality. The integration of personalized radiation risk assessment with CT dose optimization can establish safe imaging practices that comply with the fundamental ALARA (As Low As Reasonably Achievable) principle.

Nevertheless, finding the ideal balance between radiation dose and image quality remains a major clinical challenge. It is well established that using lower radiation doses reduces the possibility of adverse health effects on the patient. However, lower doses may also compromise image quality, thereby reducing the radiologist's confidence in the diagnostic value of the obtained images. Conversely, using a higher radiation dose yields superior image quality but simultaneously exposes the patient to an increased risk of radiation-induced harm. Because every patient presents varying characteristics and clinical requirements, determining an optimal, patient-specific dose that ensures both safety and reliable imaging outcomes is a complex and non-trivial problem.

The motivation for this research is directed toward improving the safety of patients who undergo medical imaging procedures, as well as reducing unnecessary radiation exposure from CT devices to lower the risk of long-term adverse health effects—especially in vulnerable populations such as pediatric patients and individuals who receive repeated CT scans. Recent technological advances, including machine learning, deep learning, and intelligent dose-tracking systems, offer new opportunities for developing personalized dose management systems and predictive models for radiation risk. Utilizing these technologies as tools to enhance patient safety, image quality, and the diagnostic value of CT examinations provides a novel pathway to ensure that CT exams deliver high diagnostic effectiveness without exposing patients to excessive radiation.

This work reviews various methods previously described in the literature to assist radiologists in assessing the risks of radiation exposure and to provide them with actionable CT dose information. The primary focus of this study is on the processes that allow radiologists to adjust the radiation dose of a CT scan for individual patients before the scan is acquired, based on parameters that are unique to each specific patient. Through simulations and data analysis, this study aims to assess whether this personalized pre-acquisition framework can decrease radiation dose while maintaining image quality. Thus, this research uses personalized risk assessment and pre-scan dose adjustment to protect patients while preserving clear, diagnostically useful images.

This thesis is organized into three main chapters:

Chapter One:presents the core concepts related to computed tomography, discusses the major types of radiation produced by CT scanners and their potential impacts on patient health, reviews major international protocols related to radiation protection, and includes clinical examples illustrating how various factors influence radiation dose for individual patients.

Chapter Two: critically reviews the evolution of CT dose optimization methods between 2015 and 2025, compares conventional and deep learning–based approaches, examines emerging strategies in personalized radiation risk assessment, and identifies the key research gaps that motivate the present study. It synthesizes dose optimization and radiation risk assessment which previous studies have largely treated as separate domains to identify integrated solutions that address both image quality preservation and patient-specific risk estimation.

Chapter Three: presents the comprehensive methodology adopted to develop an intelligent pipeline for predicting CT radiation dose (CTDIvol and DLP) and assessing personalized radiation risk in pediatric patients using machine learning techniques. It describes the dataset, preprocessing steps, data splitting strategy, feature scaling, and the four implemented machine learning models (Random Forest, Gradient Boosting, Support Vector Machine, and Multi-Layer Perceptron). The chapter then reports the experimental results for both regression tasks and the classification task, followed by a critical discussion and interpretation of the findings.

1. Physical Principles and Health Risks of Computed Tomography Imaging

1.1 Introduction

Computed tomography (CT) is one of the most important medical technologies today, as it can rapidly produce high-quality diagnostic images to meet today's medical needs. Unfortunately, the challenge associated with using CT technology is to achieve a balance between the radiation dose given to the patient and the quality of images produced. A reduction in the radiation dose can cause reduced clarity of images and affect the ability to accurately diagnose disease, whereas an increase in the radiation dose improves clarity but can put the patient at risk of exposure to ionising radiation, which can be harmful. Therefore, it is critically important to understand the basic principles of CT imaging and the risks associated with exposure to radiation.

Accordingly, the primary purpose of this chapter is to provide the basis for understanding the fundamental principles of CT imaging and to explain the types of radiation used in CT and their physical principles, as well as their biological effects on the human body. This chapter also provides the foundation for understanding the basic principles of radiation protection and the international and national guidelines developed to help establish appropriate safety standards. This thorough understanding serves as the basis for the following chapters, where radiation risk from CT examinations will be evaluated and optimal methods for improving and implementing quality control programs to minimise the radiation dose received during CT scans will be identified, thereby ensuring a balance between patient safety and diagnostic effectiveness.

1.2 Fundamentals of Ionizing Radiation in CT

1.2.1 Definition of Ionizing Radiation

Ionizing radiation is a type of radiation that has sufficient energy to eject electrons from atoms or molecules, thereby creating ions. This characteristic distinguishes ionizing radiation from non-ionizing radiation, which lacks the energy required to produce fundamental atomic or molecular changes [2, 3].

X-rays are the principal form of ionizing radiation used in computed tomography (CT) imaging. CT images are generated as X-rays penetrate biological tissues and interact with matter at the atomic scale [2]. Due to their high energy, ionizing radiations can induce molecular alterations within tissues and cells, most notably DNA damage. This damage may occur through direct interactions with DNA molecules or indirectly through the production of free radicals (highly reactive atoms or molecules with unpaired electrons that can damage DNA, proteins, and cell membranes), which can subsequently damage cellular structures [3].

These interactions create the basis for the diagnostic usefulness of CT. However, as illustrated in Figure 1.1, the high-energy levels and short wavelengths (reaching 0.01 nm to 10 nm for diagnostic X-rays) place X-rays in the ionizing radiation region of the electromagnetic spectrum. This physical positioning underscores the potential for patient exposure to radiation-related risks, as the energy exceeds the ionization threshold required to induce molecular damage.

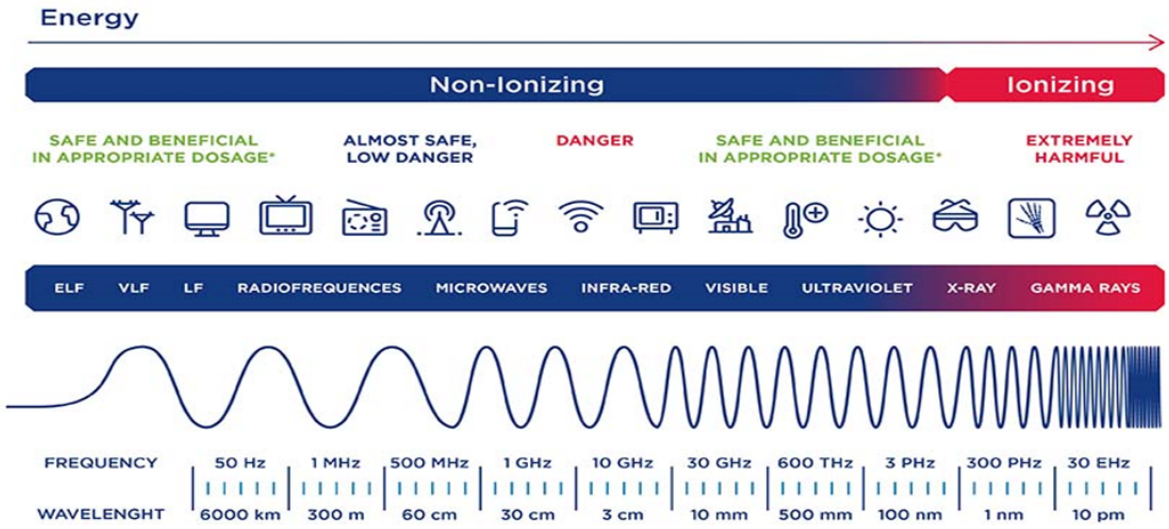

Figure 1.1: *The Electromagnetic Spectrum: From Non-Ionizing to Ionizing Radiation [1]*

1.2.2 Types of Radiation Used in CT Scans

X-ray beams used in computed tomography (CT) imaging are polychromatic beams produced from 80–140 kVp; these beams allow for fully detailed cross-sections of the human body [1]. The potential of the X-ray tube (kVp) determines the energy of the photons; higher kVp results in more penetrating photons, allowing for a lower radiation dose, though tissue contrast diminishes if the kVp is too high [4, 5]. Proper filtration removes low-energy photons that would be absorbed superficially, reducing unnecessary exposure without improving image quality [3, 5].

When X-rays interact with tissue, two fundamental mechanisms occur, as depicted in Figure 1.2, the photoelectric effect and Compton scattering [1]. The photoelectric effect occurs when a photon is completely absorbed by a bound electron, which is then ejected; this interaction increases in high-density tissues like bone, providing the basis for skeletal contrast [4]. In comparison, Compton scattering involves inelastic collisions resulting in photon deflection and partial energy loss, which is a primary source of image noise and contributes to patient dose [4].

The CT detector identifies these interactions for image reconstruction [5]. However, these interactions also produce cellular ionization, causing DNA damage and potentially leading to long-term risks such as radiation-induced cancer [2, 6]. Therefore, understanding these physical and clinical repercussions is essential for optimizing CT protocols and minimizing patient exposure [3, 2].

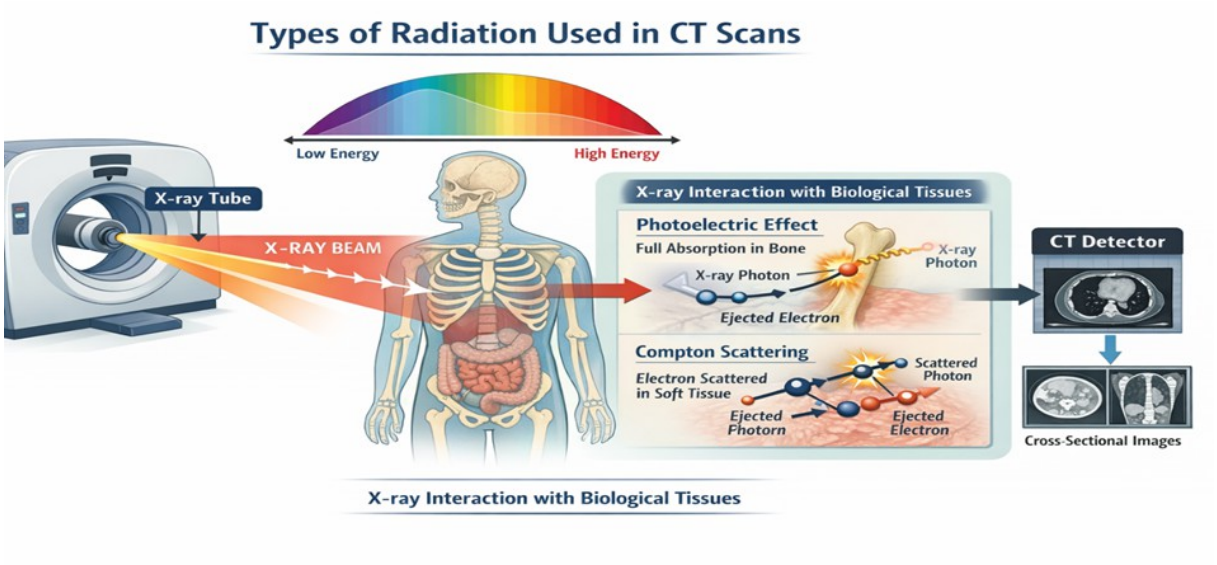

Figure 1.2: *X-ray Generation and Interaction with Biological Tissues in CT Imaging. Source: Figure by author.*

1.2.3 Production of X-rays in CT Systems

Computed Tomography, or CT, is achieved using X-ray technology. An X-ray tube produces X-rays through a process in which high-voltage electricity causes electrons released by a heated cathode to travel toward a tungsten anode, producing ionizing radiation (or X-rays) that can be processed to form a CT image [1].

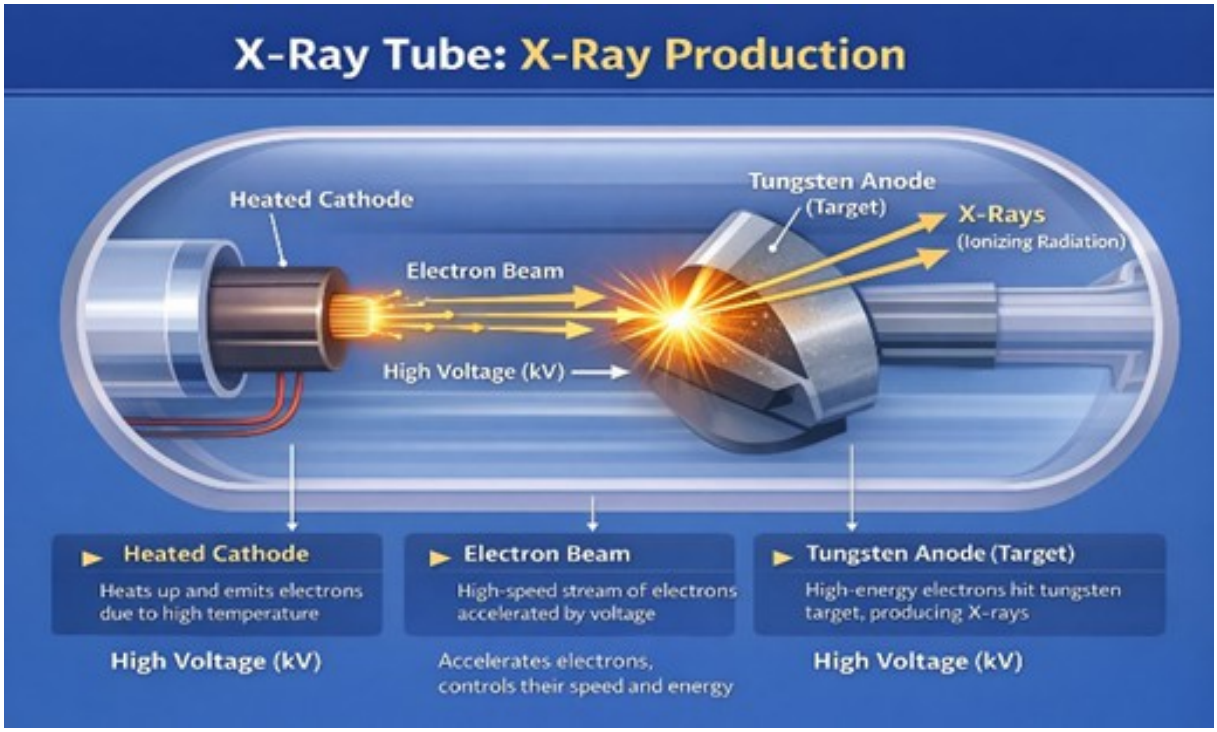

Figure 1.3: *Detailed diagram of the X-ray tube: showing the heating of the cathode, electron acceleration through high voltage, and the interaction with the tungsten anode to produce X-rays.*
Source:Figure by author

The X-ray beam is modified using filtration and collimation prior to reaching the patient. Filtration removes low-energy X-ray photons (the lowest-energy X-rays do not provide acceptable quality images), while collimation reduces the area being examined and therefore reduces the amount of unnecessary radiation delivered during the CT exam [3, 5]. Therefore, both of these functions help to minimize the overall radiation to which a patient will be subjected while retaining CT image quality [3, 5].

Finally, the production intensity of the X-ray beam at a given time and the total X-ray output during CT imaging are governed by specific technical parameters. These parameters include:

- **kVp (kilovoltage peak):** which indicates the energy penetration capabilities of the X-ray beam.
- **mA (milliamperes):** which specifies the amount of X-ray photons produced.
- **Time of rotation:** which describes how long the X-ray tube revolves around the patient's body.

Together, these parameters must be carefully adjusted to achieve an optimal balance between diagnostic image quality and radiation safety [1, 7].

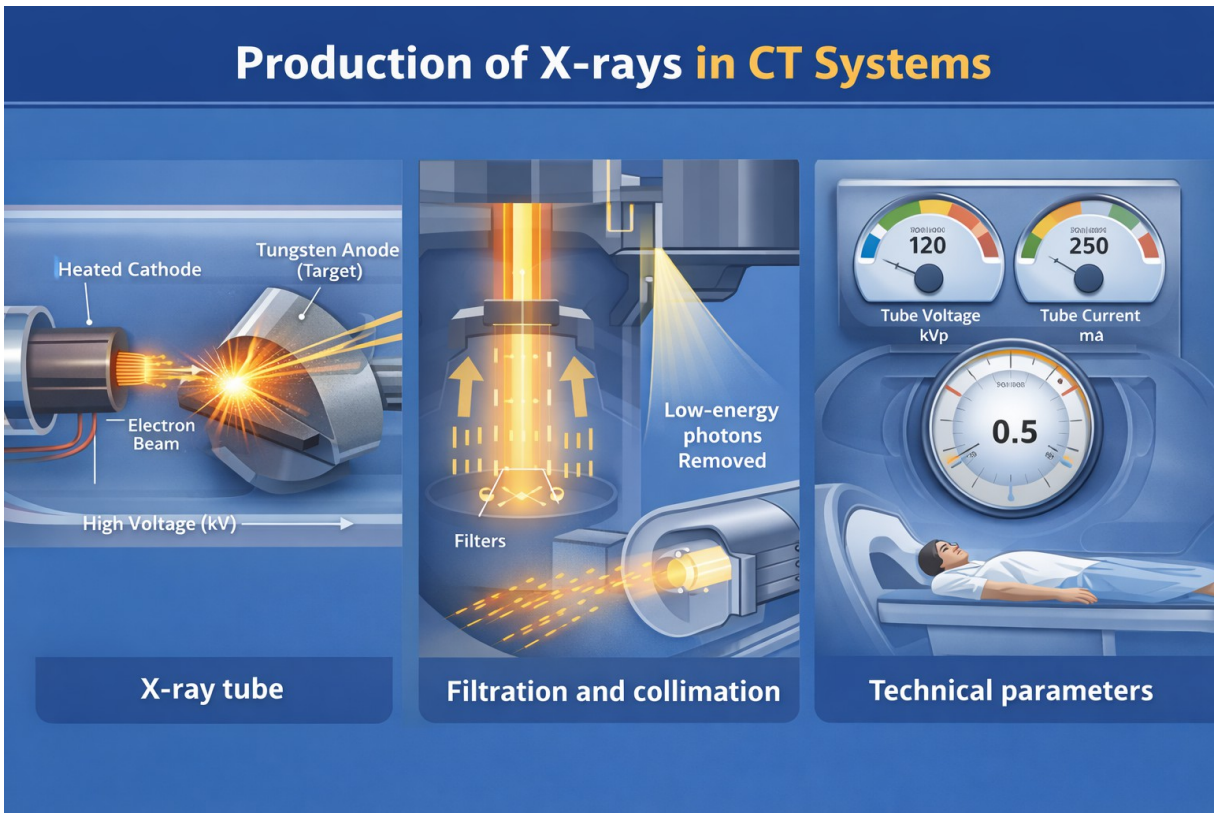

Figure 1.4: *Overview of X-ray production in CT systems: illustrating the filtration process to remove low-energy photons and the technical parameters (kVp and mA) that govern beam quality and quantity. Source:Figure by author*

1.3 Radiation Dose Metrics in CT Imaging

1.3.1 The Relationship Between Radiation Dose and Image Quality

Computed tomography uses a polychromatic x-ray tube to produce images of body cross sections. Production of these images typically requires the use of an x-ray imaging system generating x-ray tube potentials (kVp) in the range of 80 – 140 kVp [1]. The x-ray photon energy is determined by the kVp of the x-ray tube; increasing kVp provides higher penetration power of photons resulting in lower radiation dose to the patient but potentially reducing contrast of an image [5, 7]. Conversely, decreasing the kVp will improve image contrast, however higher radiation dose will be delivered to the patient [5, 7]. Effective filtration removes low-energy photons that will be absorbed at the tissue surface, thereby decreasing unnecessary radiation dose without improving image quality [3, 5].

Two mechanisms are involved when x-rays interact with human tissue: the photoelectric effect and Compton scattering [1]. The photoelectric effect occurs when a photon transfers all of its energy to a bound electron, which completely absorbs the

photon; the photoelectric effect will occur more frequently in high-density tissues (e.g., bone) compared to low-density tissue, and as such, will provide good image contrast between opaque (bone) and adjacent radiolucent (soft tissue) structures [4]. Compton scattering occurs when an inelastic collision occurs between a photon and a loosely bound electron, with the result being partial loss of energy and deflection of the photon; Compton scattering predominates in soft tissues and contributes to image noise, image scatter artifacts and the radiation dose delivered to a patient [1, 7]. All simultaneous interactions of tissue with photons are termed photon-tissue interactions other than pair production [1]. A comprehensive visual representation of the previously discussed CT physics principles, including beam energy, filtration, and photon–tissue interactions, is presented in Figure 1.5.

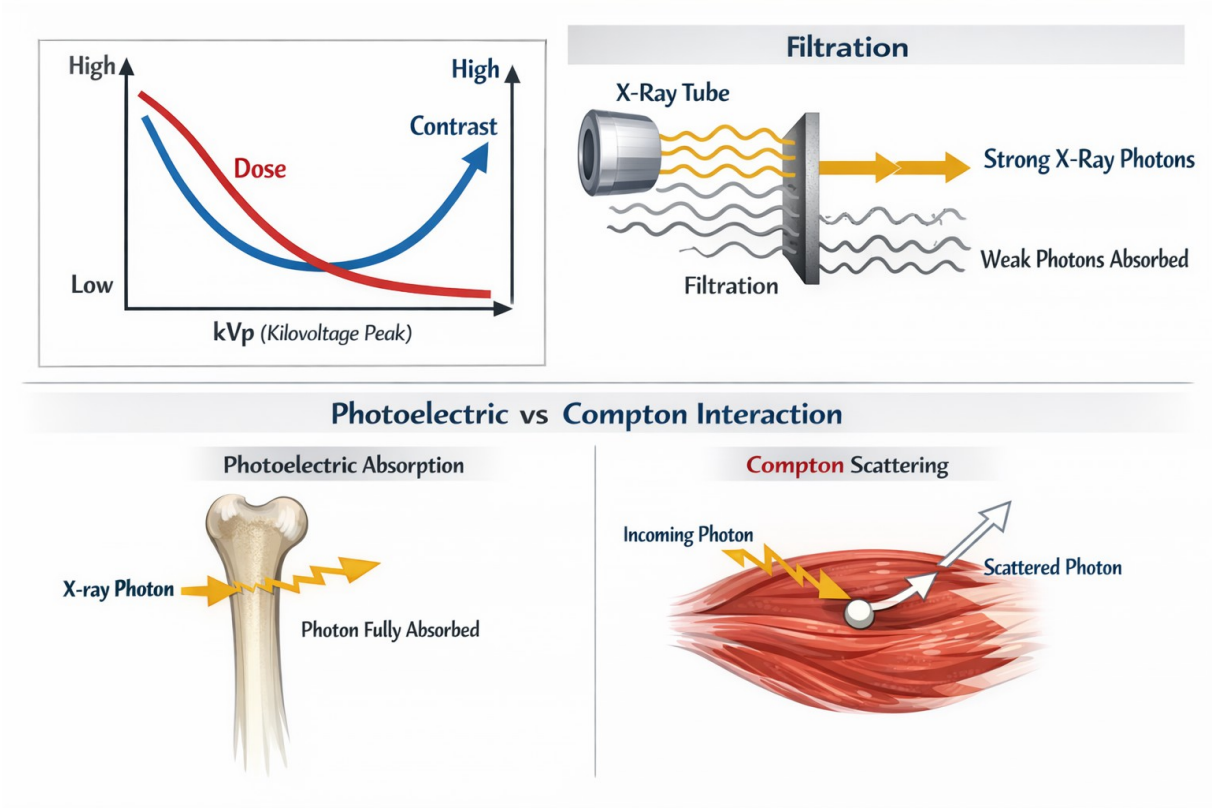

Figure 1.5: *Summary of CT physical principles: The dose-contrast relationship relative to kVp (top-left), the mechanism of beam filtration (top-right) and a comparison between Photoelectric and Compton tissue interactions (bottom). Source: Figure by author*

1.3.2 Dosimetric Quantities in CT

The Computed Tomography Dose Index (CTDI) represents the first step in estimating patient radiation dose from a CT examination. CTDI is defined as the radiation dose delivered during a single rotation of the X-ray tube under standardized reference conditions [1, 5]. In clinical practice, a more relevant metric is the Volume Computed Tomography Dose Index ($CTDI_{vol}$), which accounts for the pitch in helical CT acquisitions and provides a standardized measure of the average radiation intensity within the scanned volume using standardized phantoms [7, 5].

The next step in the dose estimation process is the Dose–Length Product (DLP), which is calculated as the product of $CTDI_{vol}$ and the scan length. DLP represents the total radiation energy delivered during a CT examination and is widely used for protocol comparison, dose auditing, and the establishment of diagnostic reference levels [3, 2]. Both $CTDI_{vol}$ and DLP are indicators of scanner output and do not directly reflect organ doses or the individual biological risk associated with a CT examination [1, 4].

Effective dose (E) provides a population-based, risk-related estimate of radiation exposure by applying tissue weighting factors that account for the different radiosensitivities of organs and tissues [2, 6]. In CT imaging, effective dose is commonly estimated from the DLP using region-specific conversion coefficients to allow approximate comparison of stochastic radiation risks, such as the risk of radiation-induced cancer, between different CT protocols and imaging modalities [7, 2]. However, effective dose is not intended for estimating radiation risk in individual patients. Nevertheless, understanding effective dose and its proper use is essential for CT protocol optimization, dose management, and the application of the ALARA (As Low As Reasonably Achievable) principle in clinical CT practice [3, 5].

1.4 Biological Effects of CT Radiation on Public Health

1.4.1 Mechanisms of Radiation Interaction with Human Cells

X-ray photons used in CT are low-LET (Linear Energy Transfer) ionizing radiation that interact with tissue by photoelectric effect and Compton scattering, producing energetic electrons that deposit energy along their tracks [6]. Two principal mechanisms of interaction with cells are distinguished [6, 2]:

- **Direct action:** Energy is deposited directly in critical biomolecules (especially DNA), causing base damage, single-strand breaks (SSBs), double-strand breaks (DSBs), and DNA–protein crosslinks. DSBs are the most consequential lesions, often leading to chromosomal aberrations and cell death or mis-repair [6, 8].
- **Indirect action:** Most cellular water is radiolysed, producing reactive oxygen species (ROS) such as OH•, H•, and hydrogen peroxide (H2 O2). These diffuse to DNA and other targets, generating oxidized bases, SSBs, and clustered DNA damage [6, 8].

Radiation-induced DNA damage activates complex DNA damage response (DDR) pathways: sensor proteins recognize lesions, trigger cell-cycle checkpoints, and recruit repair systems (non-homologous end-joining for DSBs, base excision repair for SSBs) [8]. Mis-repair can fix mutations that underlie carcinogenesis; extensive or irreparable damage can result in apoptosis, mitotic catastrophe, or senescence [6, 9]. In CT-level exposures (a few to tens of mGy per scan), the average number of DSBs per cell is small, but a large cell population is exposed, so even a low per-cell transformation probability can translate into a measurable population-level cancer risk [2, 9].

1.4.2 Deterministic Effects

Deterministic effects (the International Commission on Radiological Protection (ICRP) now terms them "tissue reactions") show a dose threshold below which they are not observed and whose severity increases with dose [2, 10, 11]. They arise when radiation kills or functionally impairs a critical number of cells in a tissue [6]. Typical approximate thresholds for low-LET radiation in humans are in the hundreds of mGy to Gray range, far above doses from a single diagnostic CT [2, 6]. Examples include:

- Skin erythema and epilation after localized doses ≥2–3 Gy during fluoroscopically guided procedures [10, 12].
- Cataract formation in the lens; the ICRP currently uses a threshold of about 0.5 Gy for protracted exposure when setting lens dose limits [2, 11].
- Bone marrow depression, gastrointestinal syndrome, and neurovascular syndrome in acute whole-body exposures at multi-Gy levels [6].

Standard diagnostic CT of a single body region (effective dose ∼2–20 mSv; corresponding organ doses ∼tens of mGy) does not cause immediate deterministic injury in patients with normal tissue tolerance [13, 12]. However, repeated high-dose or interventional CT-guided procedures can approach thresholds in localized tissues, reinforcing the need for careful protocol selection and monitoring of cumulative organ doses in high-use scenarios [13, 12, 9].

1.4.3 Stochastic Effects

Stochastic effects are random in occurrence: their probability (but not severity) increases with dose, and no dose threshold is assumed [2, 10, 11]. The principal stochastic outcomes associated with CT X-rays are radiation-induced cancers and, to a much lesser extent in humans, heritable effects [2, 6]. Epidemiological evidence derived from atomic-bomb survivors, as well as medically and occupationally exposed populations, supports an approximately linear dose–risk relationship for solid cancers and leukemia down to doses of at least several tens of mGy [10, 2].

On this basis, international radiation protection bodies have adopted the Linear No-Threshold (LNT) model, which assumes that any incremental dose of ionizing radiation, regardless of magnitude, results in a proportional increase in cancer risk [2, 10]. The LNT model underpins the ICRP's derivation of detriment-adjusted nominal risk coefficients and the establishment of effective dose limits for occupationally exposed workers and the general public [2].

Some radiobiological and modeling studies suggest that low-dose responses may deviate from strict linearity and that adaptive responses or dose-rate effects could imply effective thresholds or nonlinear behavior [11]. Nevertheless, for regulatory and public health purposes, the LNT model remains the conservative reference framework adopted by the ICRP, International Atomic Energy Agency (IAEA), and major professional societies for estimating CT-related cancer risk and guiding dose optimization strategies [2, 10, 11].

1.4.4 Impact of CT Radiation on Public Health

The global use of computed tomography (CT) has expanded dramatically since its introduction, making CT the dominant contributor to the collective effective dose from

medical X-ray imaging worldwide [13, 12, 9]. Typical adult CT examinations deliver effective doses on the order of a few to several tens of mSv, substantially higher than those associated with conventional radiographic procedures [13, 12].

Population-based analyses have linked the increasing utilization of CT to a marked rise in collective radiation dose, raising concerns regarding future CT-attributable cancers, particularly when examinations are repeated over extended periods of time [12, 9, 13].

Children represent a particularly radiosensitive population due to their rapidly dividing tissues, higher organ doses for equivalent CT techniques, and longer post-exposure life expectancy [10, 12, 9]. Several large cohort studies of pediatric CT have demonstrated positive dose–response relationships for leukemia, brain tumors, and other malignancies at cumulative organ doses of a few tens of mGy, suggesting small but measurable absolute risks at the population level [12, 9, 13].

Pregnant women and the developing fetus are also considered populations of special concern. Fetal radiosensitivity varies according to gestational age; although deterministic effects require radiation doses far exceeding those delivered by optimized maternal CT examinations, potential stochastic risks, such as childhood cancer, justify stringent justification criteria and a preference for non-ionizing imaging modalities whenever feasible [2, 10, 12]. International recommendations therefore emphasize careful risk–benefit communication and the adjustment of CT protocols to patient-specific conditions when imaging is clinically indispensable [2, 10, 12].

1.5 International Radiation Protection Protocols and Guidelines

1.5.1 ALARA Principle in CT Imaging

Modern radiation protection is founded on the triad of justification, optimization, and dose limitation, commonly summarized by the ALARA (As Low As Reasonably Achievable) principle [2, 3].

Justification: Any CT examination must provide a net clinical or public health benefit. Unindicated or duplicative scans should be avoided, and alternative non-ionizing imaging modalities such as ultrasound or magnetic resonance imaging (MRI) should be preferred when they can provide diagnostically adequate information [2, 3, 12].

Optimization: For examinations that are clinically justified, imaging parameters including tube voltage (kV), tube current (mA), pitch, collimation, scan length, and reconstruction algorithms are tailored to achieve sufficient diagnostic image quality at the lowest reasonable radiation dose. This process relies on diagnostic reference levels (DRLs) as well as size- or age-based protocols, particularly for pediatric populations [2, 3, 12, 9].

Dose limitation: Numerical dose limits apply to occupationally exposed workers and members of the public, but not to patients undergoing medically justified diagnostic CT examinations. Nevertheless, dose limits for staff and the public in and around CT facilities, including limits for lens and skin exposure, inform shielding requirements and procedural design [2, 11]. For patients, dose constraints and diagnostic reference levels are applied within the framework of optimization rather than strict regulatory limits [2, 3].

1.5.2 International Organizations and Recommendations

Several international organizations provide authoritative guidance relevant to radiation protection in CT imaging:

- **International Commission on Radiological Protection (ICRP):** Issues foundational recommendations, such as ICRP Publication 103, defining core radiation protection principles, dose quantities, tissue weighting factors, and nominal risk coefficients that underpin effective dose calculations as well as justification and optimization strategies in CT practice [2].
- **International Atomic Energy Agency (IAEA):** Publishes the International Basic Safety Standards (GSR Part 3), which harmonize regulatory requirements worldwide for medical, occupational, and public exposures. These standards emphasize justification, optimization, quality assurance, and education in CT practice [3].
- **World Health Organization (WHO):** Promotes patient safety in medical imaging, encourages the use of appropriateness criteria and dose tracking, and collaborates with the IAEA and ICRP in initiatives aimed at reducing unnecessary radiation exposure, particularly in children and pregnant women [12, 14, 15].
- **American Association of Physicists in Medicine (AAPM):** Produces detailed reports and task-group guidelines addressing CT dosimetry, scanner performance, and protocol optimization for both adult and pediatric imaging, including the application of $\mathrm{CTDI_{vol}}$, dose-length product (DLP), and size-specific dose estimates (SSDE) [13, 16].
- **European guidelines:** European professional and regulatory bodies adapt ICRP and IAEA recommendations into region-specific CT guidelines and diagnostic reference levels, with particular emphasis on pediatric imaging, structured justification pathways, and rigorous quality control programs [12, 17].

Together, these international organizations shape national regulations, accreditation frameworks, and clinical practice guidelines, thereby promoting safer, more consistent, and more optimized use of CT imaging worldwide.

1.5.3 Relationship Between Delivered Dose and Patient Parameters

The radiation dose received by a patient during a CT examination depends not only on scanner settings but also on patient-related parameters and the anatomical region being imaged [13, 12, 8, 9].

- **Age:** Children and small adults absorb higher organ doses for the same $\mathrm{CTDI_{vol}}$ (Volume CT Dose Index) owing to smaller body diameters and reduced photon attenuation, resulting in an increased lifetime attributable cancer risk. Consequently, pediatric CT protocols typically employ reduced tube voltage and current and restrict scan length to the minimum required for diagnostic purposes [10, 13, 12, 9].

- **Sex:** For an equivalent absorbed organ dose, females generally exhibit higher effective radiation risk because radiosensitive organs such as the breast and thyroid are assigned larger tissue weighting factors. CT protocol design therefore places particular emphasis on minimizing exposure of the breast and gonads, including exclusion from the primary beam or shielding when clinically feasible [10, 11, 9].

- **Body weight, BMI, and morphology:** Larger patients require higher tube current or tube voltage to maintain acceptable image quality, leading to increased radiation dose. Conversely, smaller or leaner patients can often be imaged using substantially reduced exposure parameters. Automated tube current modulation systems dynamically adapt tube output to patient cross-sectional size and attenuation characteristics [13, 8, 9].

- **Anatomical region examined:** Organ doses and associated radiation risks vary considerably among head, chest, abdominal–pelvic, and cardiac CT examinations. Radiosensitive tissues, including bone marrow, breast, lungs, thyroid, and gonads, may receive substantial doses depending on the scanned region and imaging protocol [10, 13, 12, 8, 9].

Understanding these relationships is essential for patient-specific CT protocol selection, accurate radiation risk estimation, and effective risk communication in clinical practice.

1.6 Personalized Radiation Risk Assessment

1.6.1 Concept of Personalized Medicine in Medical Imaging

Conventional CT practice has historically relied on standardized imaging protocols defined primarily by anatomical region, with limited consideration of inter-individual variability. However, advances in CT technology, dosimetry, and radiobiology, together with increasing awareness of the potential risks associated with low-dose ionizing radiation, have driven a progressive shift toward personalized, patient-specific imaging protocols [13, 12, 9].

Personalized CT imaging integrates multiple patient- and indication-specific factors, including:

- **Age- and size-adapted exposure parameters:** Adjustment of tube voltage and tube current according to patient age and body habitus (e.g., pediatric versus adult patients, small versus large body size) to ensure adequate image quality at the lowest reasonable radiation dose.

- **Clinical question–driven scan design:** Optimization of scan length, number of acquisition phases (e.g., pre- and post-contrast), and scan coverage strictly according to the diagnostic task, thereby avoiding unnecessary multiphase examinations when not clinically justified.

- **Advanced image reconstruction techniques:** Application of iterative reconstruction and noise-optimized acquisition protocols to preserve diagnostic image quality while enabling substantial dose reduction.

- **Individual radiation risk considerations:** Incorporation of patient-specific risk factors, such as young age, known or suspected genetic radiosensitivity, and limited remaining life expectancy, when balancing diagnostic benefit against radiation risk and when selecting the most appropriate imaging modality [10, 13, 12, 9].

This paradigm shift aligns CT practice with the broader principles of personalized medicine, aiming to maximize diagnostic and therapeutic benefit while minimizing potential harm at the level of the individual patient rather than an average "standard" patient.

1.6.2 Patient-Specific Risk Factors

Personalized radiation risk assessment in CT imaging considers multiple patient-specific factors that extend beyond the parameters of the immediate examination.

- **Prior radiation exposure history:** Previous exposures from CT scans, interventional radiology procedures, radiotherapy, or occupational sources contribute to cumulative organ doses. In patients anticipated to undergo repeated imaging over time, such as those with chronic diseases or requiring cancer follow-up, minimizing dose per examination and considering alternative non-ionizing imaging modalities becomes particularly important [10, 12, 9].
- **Biological sensitivity:** Certain populations, including children, pregnant women, and individuals with DNA repair deficiencies or other radiosensitivity conditions, exhibit increased susceptibility to stochastic effects and, potentially, tissue reactions at a given radiation dose. In these groups, lower thresholds for switching to ultrasound or MRI, and more aggressive dose optimization strategies, are warranted [10, 12].
- **Remaining lifetime expectancy:** For patients with long anticipated survival (e.g., pediatric and young adult populations), even small incremental radiation risks may accumulate over decades. Conversely, in patients with limited life expectancy due to advanced malignancy, the immediate diagnostic or therapeutic benefit may outweigh small long-term risk increments, justifying higher or repeated CT doses when clinically indicated [10, 12, 9].

Integration of these patient-specific risk factors supports individualized justification and optimization of CT examinations, enhances informed consent, and frames imaging decisions within a long-term survivorship and patient-centered care perspective.

1.7 Clinical Case Examples: CT Imaging in Cancer Patients

1.7.1 Role of CT in Cancer Diagnosis and Follow-up

Computed tomography (CT) plays a central role in modern oncologic imaging, providing high-resolution, cross-sectional visualization of primary tumors, nodal involvement, and distant metastases [13, 12, 9]. Typical clinical applications include:

- **Initial diagnosis and staging:** Chest, abdominal–pelvic, and neck CT examinations are used to determine TNM (Tumor, Node, Metastasis) stage in many malignancies, guiding prognosis assessment and informing therapeutic planning, including surgical resection, radiotherapy field design, and systemic therapy selection [13, 12, 9].

- **Therapeutic monitoring:** Serial CT imaging enables quantification of changes in tumor size and morphology in response to chemotherapy, targeted therapy, or immunotherapy. Standardized criteria such as RECIST (Response Evaluation Criteria in Solid Tumors) are applied, and CT can also detect treatment-related complications, including pneumonitis or gastrointestinal perforation [13, 12, 9].

- **Surveillance:** Periodic CT scans following curative-intent therapy monitor for disease recurrence or the development of new primary malignancies. This surveillance is often conducted over many years in high-risk patient populations [13, 12, 9].

While these clinical applications confer substantial diagnostic and therapeutic benefits, repeated CT examinations contribute to the accumulation of high cumulative medical radiation doses, placing cancer patients among those with the greatest lifetime exposure from medical imaging.

1.7.2 Radiation Risk in Oncologic Patients: Repeated Examinations and Dose Accumulation

Oncologic patients frequently undergo multiple CT examinations throughout the course of their disease, including initial staging, interim response assessment, restaging at progression, and post-treatment surveillance [13, 12, 9]. Each CT scan contributes organ doses on the order of tens of milligray (mGy), which can cumulatively approach or exceed levels associated with a small but measurable increase in the risk of secondary solid cancers or leukemia, particularly in long-term survivors treated at young ages [12, 9].

Cancer patients may also receive therapeutic radiotherapy, further increasing radiation dose to organs adjacent to treatment fields. Although the immediate risk–benefit balance strongly favors imaging and therapy in life-threatening malignancies, awareness of cumulative exposure supports the adoption of strategies to minimize unnecessary radiation, including:

- Preferential use of limited-range, single-phase CT protocols when clinically acceptable.

- Periodic re-evaluation of the necessity and timing of surveillance scans.

- Increased reliance on non-ionizing imaging modalities such as MRI or ultrasound for follow-up where diagnostically feasible.

These dose-reduction strategies are particularly important for pediatric and adolescent oncologic patients, who typically have high survival rates and long remaining lifetimes, thereby increasing the potential impact of cumulative radiation exposure [10, 12, 9].

1.7.3 Example of a Cancer Patient Undergoing Multiple CT Scans

Consider a 45-year-old woman diagnosed with locally advanced colorectal cancer. Her imaging course includes:

- Contrast-enhanced CT of the chest, abdomen, and pelvis for initial staging.
- CT-based radiotherapy planning of the pelvis.

During neoadjuvant chemoradiotherapy and postoperative chemotherapy, she undergoes serial abdominal–pelvic CT scans every 3–4 months to monitor treatment response and detect complications, followed by annual surveillance CT for at least five years. Over this period, she may receive approximately 10–15 body CT examinations, each with an effective dose of roughly 8–15 mSv, resulting in a cumulative effective dose on the order of 100–150 mSv, with organ doses to the bowel, bone marrow, and ovaries in the several hundred milligray range [13, 12, 8, 9].

From a public health and radiation protection perspective, this case illustrates several key principles:

- **Dose evaluation:** Use of $\mathrm{CTDI}_{\mathrm{vol}}$, DLP (Dose-Length Product), and organ dose estimation tools (based on scanner output and patient size) to quantify cumulative exposure and support informed discussions with the patient [13, 8].
- **Clinical justification:** Each examination is justified by substantial expected benefit, including accurate staging, early detection of recurrence, and management of therapy-related morbidity. Omitting critical scans could compromise prognosis [13, 12, 9].
- **Personalized dose optimization:** CT protocols are adapted to her body habitus and clinical needs, including lower tube voltage for smaller patients, automated tube current modulation, restricted z-axis coverage to the region of interest, single-phase imaging when multiphase is unnecessary, and iterative reconstruction to maintain image quality at reduced dose. When feasible, MRI or ultrasound substitutes for CT in specific follow-up scenarios (e.g., evaluation of pelvic recurrence or liver metastases) [13, 12, 8, 9].

Through such individualized balancing of diagnostic yield and radiation risk, CT can continue to play a central role in cancer care while adhering to international radiation protection principles and minimizing avoidable long-term harm.

1.8 Conclusion

In this chapter, we covered the physical and biological aspects of ionizing radiation in CT and discussed some of the potential risks to both the individual cell and the clinical environment. The relationship between the radiation output of a CT unit (CTDI) and its biological effect on a patient (effective dose) confirms the need for protection of patients and the application of the ALARA principle.

However, the identification of various risks is just the starting point; the more significant challenge is to reduce those risks while maintaining diagnostic quality. The next chapter will explore how advanced technology, specifically Artificial Intelligence, can help achieve a balance between patient safety and image quality by providing practical solutions that consider dose as well as other factors to reduce risks.

2. State of the Art

2.1 Introduction

The use of Computed Tomography (CT) has become an integral component of modern diagnostic practice due to its ability to generate high-resolution images with rapid acquisition times. However, the growing reliance on CT examinations has led to a significant increase in population-level exposure to ionizing radiation, thereby renewing concerns regarding potential long-term biological and stochastic effects.

Over the past decade, substantial progress has been made in CT dose optimization strategies. Early approaches primarily relied on hardware advancements and physics based reconstruction algorithms. More recently, technological innovations such as photon counting detectors and the integration of Artificial Intelligence (AI) have transformed CT imaging into a data-driven and adaptive system. Concurrently, international radiation protection frameworks have evolved from generalized population-based dose limits toward more individualized and patient-centered optimization models.

Despite these advancements, a fundamental challenge persists: achieving meaningful radiation dose reduction without compromising diagnostic image quality. Conventional optimization techniques are approaching intrinsic physical and noise-related limitations. Although AI-based models have demonstrated promising performance in image reconstruction and denoising, important questions remain regarding their robustness, generalizability across diverse clinical settings, and long term clinical reliability.

This chapter critically reviews the evolution of CT dose optimization methods between 2015 and 2025, compares conventional and deep learning–based approaches, examines emerging strategies in personalized radiation risk assessment, and identifies the key research gaps that motivate the present study. However, most previous studies have treated dose optimization and radiation risk assessment as separate research domains. This chapter synthesizes these two perspectives to identify integrated solutions that address both image quality preservation and patient-specific risk estimation.

2.2 Evolution of CT Dose Optimization (2015–2025)

The past decade has witnessed a paradigm shift in Computed Tomography (CT) dose optimization, driven by rapid technological advancements and a heightened awareness of radiation safety. Between 2015 and 2025, the field transitioned from conventional physics-based and hardware-centric methodologies toward autonomous, data-driven frameworks. This evolution is characterized by three pivotal phases: the refinement of traditional hardware [18], the emergence of quantum technological leaps such as photon-counting detectors [19, 20, 21], and the current era of Artificial Intelligence (AI) integration in both acquisition and reconstruction [22]. In CT imaging, reconstruction refers to the mathematical process of converting raw X-ray attenuation data (sinograms) into cross-sectional images.

2.2.1 The Pre-AI Era

Before the widespread adoption of artificial intelligence (AI) to control the radiation dose administered to patients during computed tomography (CT) scans, there were numerous strategies aimed at limiting this dose, which relied on improvements in photon detection equipment and the development of advanced reconstruction algorithms grounded in physical models [18]. The principal strategies included:

- **Automatic Tube Current Modulation (ATCM):** ATCM used patient characteristics related to attenuation to dynamically modify tube current [18].
- **Peak Kilovoltage (kVp) Adaptation:** The kVp used for CT examinations was adjusted according to patient size and the purpose of the CT acquisition [18].
- **Spectral Shaping Technologies:** Use of techniques, such as tin filtration, to eliminate low-energy photons from the CT X-ray beam that did not improve image quality but did increase patient dose [18].
- **Iterative Reconstruction (IR):** A series of methods evolved from hybrid statistical models toward more complex Model-Based Iterative Reconstruction (MBIR). While MBIR significantly improved diagnostic image quality and reduced noise compared to traditional filtered back projection (FBP), its widespread clinical adoption was hindered by substantial computational demands and prolonged reconstruction times [18].

Each of these methods resulted in moderate patient dose reductions for CT, typically in the range of 20% to 50%, while maintaining diagnostic image quality [18]. However, all of these methods were limited in their effectiveness to further reduce dose due to the inherent physical and statistical noise limitations of the photon detection and signal processing involved in making CT images. As the dose to the patient decreased, the decrease in visible image quality from quantum noise became increasingly difficult to mitigate solely by using traditional reconstruction models.

Therefore, by the late 2010s, it was clear that traditional CT optimization methods were nearing an effective ”noise-floor” barrier, meaning that further dose reduction would compromise image quality due to quantum noise [18].

2.2.2 Technological Quantum Leaps

The photon-counting computed tomography (PCCT) systems represent a paradigm shift in dose-efficient imaging. Unlike traditional energy-integrating detectors (EID), which aggregate the total energy of X-rays into a single signal, photon-counting detectors (PCD) process each X-ray photon individually and categorize it according to its specific energy level [19, 20]. The principal advantages of this technology include improved signal-to-noise ratio (SNR), intrinsic spectral imaging capabilities, reduction of electronic noise, and higher spatial resolution [19, 21].

The development of advanced high-resolution detector architectures and more efficient collimation techniques has also greatly improved the efficiency of photon utilization, enabling better contrast, reduced radiation exposure, and the potential for quantitative imaging [21].

Despite these hardware advances, the limitations of the trade-off between aggressive dose reduction and diagnostic reliability have not been fully resolved through hardware innovations alone. Consequently, increasing attention has been directed toward computational intelligence approaches, particularly artificial intelligence, as a complementary solution for CT dose optimization and image reconstruction [22].

2.2.3 Integration of Artificial Intelligence

Initially, computer-aided diagnosis (CAD) systems were primarily developed for detecting and classifying lesions after image acquisition. More recently, artificial intelligence has been integrated not only into post-processing tasks but also into image acquisition and reconstruction stages [18].

Deep learning techniques, particularly convolutional neural networks (CNNs), have demonstrated excellent performance in denoising low-dose CT scans and reconstructing images. These models are capable of learning complex relationships between low-dose and standard-dose images, allowing substantial noise reduction while preserving important structural details [22, 23].

Currently, AI has been incorporated into several aspects of CT imaging, including:

- Deep Learning Reconstruction (DLR) engines integrated into commercial CT scanners.
- Automated protocol selection systems that analyze patient morphology to determine appropriate acquisition parameters such as kVp and mAs.
- Predictive modelling approaches used to estimate optimal acquisition parameters before the scan is performed.

These developments indicate a transition in medical imaging from static rule-based optimization, where identical protocols are applied to all patients, toward adaptive data-driven imaging systems.

However, challenges remain, including the generalisability of AI models, the risk of bias within training datasets, and the necessity for extensive long-term clinical validation before widespread adoption [22].

2.3 Dose Optimization Methods

2.3.1 Conventional and Hardware-Based Methods

Dose optimization methods in computed tomography (CT) are generally based on the development of imaging hardware and physics-based reconstruction algorithms [7, 24]. A major aspect of these methods is Automatic Tube Current Modulation (ATCM), which automatically varies the tube current (mAs) according to the attenuation of the X-ray beam as it passes through the patient [24]. This results in higher exposure in denser anatomical regions and lower exposure in less attenuating areas, thereby improving image quality uniformity while minimizing unnecessary radiation dose.

At the same time, peak kilovoltage (kVp) is adjusted according to patient size and the clinical purpose of the CT examination [24]. Lower kVp values can improve iodine contrast while simultaneously reducing the overall radiation dose. In addition, spectral shaping techniques, such as the use of tin (Sn) filters, are employed to remove low-energy photons that contribute to patient dose without improving image quality [24].

In parallel with acquisition techniques, reconstruction algorithms have also evolved significantly. Iterative Reconstruction (IR) methods have largely replaced conventional Filtered Back Projection (FBP) in many modern CT systems [7]. Advanced techniques such as Model-Based Iterative Reconstruction (MBIR) can produce high-quality images

with significantly reduced noise, especially at lower dose levels [7]. However, these methods may require substantial computational resources and longer reconstruction times. Despite these advances, traditional hardware and physics-based optimization approaches are approaching fundamental statistical limits related to photon noise, often referred to as the "noise floor," particularly at ultra-low radiation dose levels [24].

2.3.2 Deep Learning-Based Optimization (The AI Frontier)

Deep learning (DL) technology has given rise to an entirely new area in improving low-dose (LD) computed tomography (CT) imaging. This is made possible by the ability of DL models to extract high-level structures from large amounts of medical data. By learning from high-quality reference data, DL can generate diagnostic-quality images using sparse or noisy input image data [18].

As related to LDCT denoising and reconstruction, a primary architecture used is Convolutional Neural Networks (CNNs). CNNs complete the non-linear mapping process from the original noisy LDCT acquisition to a standard dose CT acquisition while suppressing quantum noise and maintaining anatomical detail faithfully [22].

Additionally, Generative Adversarial Networks (GANs) show great potential value in LDCT imaging. GANs utilize a two-part network system: the Generator synthesizes CT images, while the Discriminator evaluates the generated image's authenticity. As a result, when used with ultra-low-dose CT acquisition data, GANs provide reconstructed high-quality CT images with realistic texture and detail compared to more traditional reconstruction methods [22].

The growing amount of AI and ML for clinical use in medical imaging has dramatically increased with the advent of commercial Deep Learning Reconstruction (DLR) systems. Major CT manufacturers now include standalone AI engines built directly into the acquisition processes of their scanners. Examples include GE's TrueFidelity™ and Canon Medical's AiCE, which utilize deep neural networks to perform advanced reconstruction and produce high-fidelity images even at significantly reduced dose levels [18].

In addition to reconstruction, AI is also increasingly used to automate and optimize scanning protocols. AI-based systems analyze scout images and patient anatomy to determine parameters such as kVp and mAs, enabling a transition from non-adaptive to adaptive and personalized CT acquisition strategies [22].

2.3.3 Personalized Radiation Risk Assessment

Traditional methods for optimizing doses from imaging have focused on decreasing the amount of radiation used during imaging procedures. Recent research has demonstrated the need for an individual-based (or personalized) approach to radiation risk assessments [13, 9].

Estimations of radiation risks based on standard metrics (e.g., effective dose) provide only rough estimates since they do not reflect patient-specific anatomical and biological variations [2, 3].

To help overcome this limitation, new methods utilize organ-specific dose estimations, which measure the radiation dose to individual organs rather than population averages. Modern simulations rely heavily upon computer-based models (e.g., voxel-based phantoms and NURBS phantoms) [13, 9].

Certain patient-specific characteristics (e.g., age, gender, BMI(the weight), and heritable risk) also significantly affect radiation response and long-term cancer risk [13, 9]. Incorporating this information in dose estimation models improves accuracy and enables better personalized dose assessments.

Recent developments in artificial intelligence (AI) have enabled predictive models for radiation-induced cancer risk, using clinical and dosimetry databases to estimate future risks following imaging studies. Personalized radiation risk assessments are becoming a key element of contemporary CT safety [2, 3].

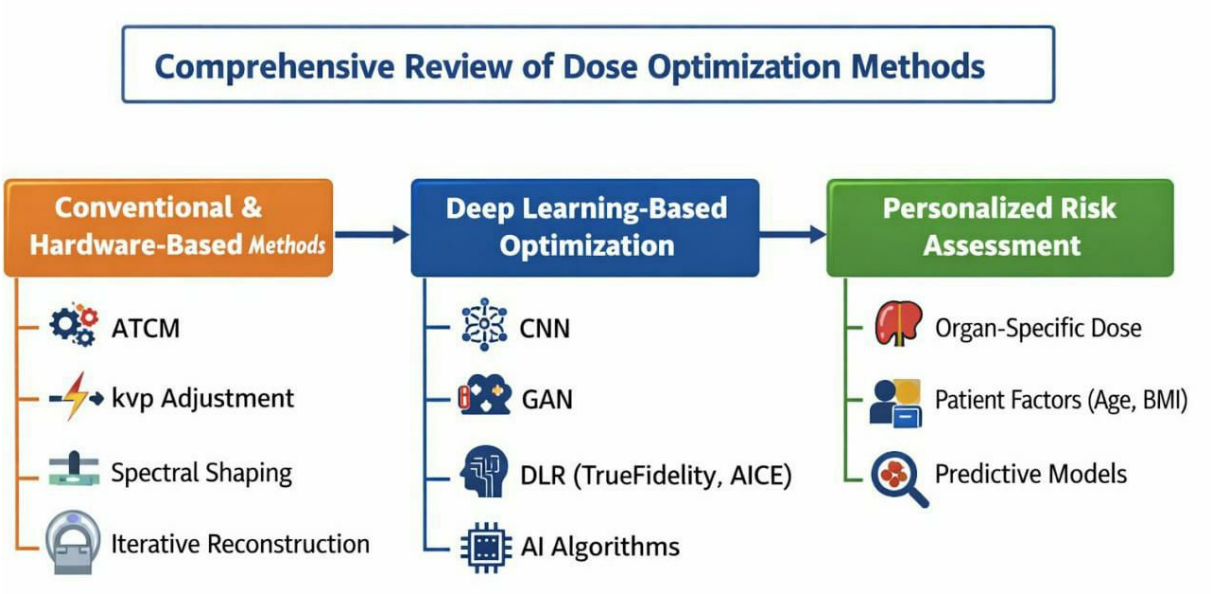

Figure 2.1: *Conceptual classification of CT dose optimization methods. Source: Figure by author.*

2.4 Comparative Analysis of DL-based Optimization

Artificial Intelligence (AI) has become an essential facet of Computed Tomography (CT) due to its ability to provide reliable and reproducible predicted radiation dose metrics for quality assurance, as well as its ability to produce high-quality images using Deep Learning Reconstruction (DLR). Several studies have investigated the potential of AI for dose prediction, image quality optimization, and reconstruction. Table 2.1 summarizes the key characteristics and findings of these studies, including the types of datasets, AI models employed, and main results achieved.

Table 2.1: *Summary of AI-based approaches for CT dose prediction and image quality optimization*

Reference & Study	**Year**	**Objective & Key Findings**	**Dataset**	**AI Model**
[25]: Meineke et al.	2019	Detect dose optimization potential in chest CT QA. Successfully identified exams exceeding predicted CTDIvol thresholds	3,199 chest CT examinations	Feed-forward neural network
[26]: Tekin et al. (Abdomen)	2022	Predict DLP for abdominal CT. Bayesian algorithm showed superior performance (R = 0.957)	551 abdominal CT datasets	ANN (Bayesian)
[27]: Tamura et al.	2022	Compare low-dose DLR with HIR. Low-dose DLR maintained image quality with lower exposure	71 patients	Deep Learning (AiCE)
[28]: Park et al.	2022	Assess DLR at different tube voltages. Dose reduction up to 61.5%	1 abdominal phantom	Deep Learning (TrueFidelity)
[29]: Moradmand et al.	2023	Predict breast dose in chest CT using ANFIS. Achieved R = 0.93 correlation	50 patients	ANFIS
[30]: Liu et al.	2024	Evaluate AI with low-dose chest CT. 65% dose reduction with improved quality	100 patients	Deep learning algorithm

2.4.1 Quantitative Comparison

The quantitative analysis of the provided studies reveals a transformative capacity for radiation dose reduction through AI-driven interventions. Rather than marginal gains, the integration of Deep Learning Reconstruction (DLR) has enabled a substantial decrease in exposure levels. Specifically, Liu et al. [30] achieved a 65% reduction in $CTDI_{vol}$ by transitioning from standard protocols to AI-combined low-dose settings. Similarly, Park et al. [28] demonstrated that DLR can maintain superior noise control even when operating at only 38.5% of the routine dose (a 61.5% reduction), effectively outperforming traditional Hybrid Iterative Reconstruction (HIR) at full exposure. This trend is further supported by Tamura et al. [27], who reported a 40.6% significant decrease in the total effective dose ($P < 0.001$,0.1% probability of random chance), indicating that this reduction was statistically significant and highly unlikely to be due to random variation.

Regarding predictive precision, the performance of Artificial Neural Networks (ANNs) and hybrid models remains exceptionally high across different anatomical regions. Moradmand et al. [29] achieved a correlation coefficient of R = 0.93 for predicting breast dose in chest CT using an Adaptive Neuro-Fuzzy Inference System (ANFIS). Similarly, Tekin et al. (Abdomen) [26] reported predictive accuracy rates exceeding 95% for abdominal scans, proving that parameters such as BMI and age are highly reliable predictors for personalized dosing. Furthermore, the sensitivity of these models in identifying dose optimization opportunities reached 83%, with a relatively low margin of error (RMSE of 1.76 mGy) [25].

Finally, the balance between dose reduction and image quality has shifted in favor of AI models. Subjective quality assessments indicate that AI-optimized protocols do not just "maintain" quality but can actually improve it by approximately 17.5% compared to routine high-dose protocols [30]. This is evidenced by higher Contrast-to-Noise Ratios (CNR) even at lower tube voltages (80 kVp), where DLR models surpassed the performance of traditional HIR at higher energy levels (120 kVp) [28].

2.4.2 Research Gaps Identification

Despite recent progress in the application of Artificial Intelligence (AI) for radiation dose optimization in Computed Tomography (CT), several gaps remain in the scientific literature:

1. **Limited Use of Comprehensive Anthropometric Parameters**

   Many AI-based models rely on a limited number of anthropometric parameters, most commonly Body Mass Index (BMI) or body weight, for radiation dose prediction. Studies conducted by Tekin et al. [26] and Meineke et al. [25] demonstrate the feasibility of using these parameters for dose estimation. However, the reviewed studies rarely incorporate a comprehensive set of patient-specific variables such as height, sex, and water-equivalent diameter simultaneously for automated protocol optimization.

2. **Focus on Post-Scan Image Reconstruction Rather Than Prospective Optimization**

   A large proportion of the literature focuses on improving image quality after image acquisition through advanced reconstruction techniques. Deep learning reconstruction methods have been shown to reduce noise and maintain diagnostic

image quality at lower radiation doses, as reported by Tamura et al. [27], Park et al. [28], and Liu et al. [30]. In contrast, fewer studies investigate the use of AI for prospective optimization, such as recommending optimal tube voltage (kVp) and tube current (mAs) settings before the CT examination.

3. **Limited Generalizability of Current AI Models**

   Another limitation observed in the reviewed studies is the restricted diversity of training datasets. Many AI models are developed using data collected from a single institution or from specific imaging systems. As indicated in studies on dose prediction using artificial neural networks [26], additional validation using larger and multi-institutional datasets would be necessary to improve the robustness and generalizability of AI-based dose prediction models.

4. **Limited Interpretability and the "Black-Box" Nature of Models**

   Although deep learning techniques have demonstrated promising results in dose optimization, their decision-making processes often suffer from the "black-box" nature of deep learning architectures. Most of the reviewed studies focus mainly on model performance and predictive accuracy, while the explainability (XAI) of these systems—essential for clinical trust and safety—remains a challenge [22]. Integrating these models into routine clinical workflows requires further investigation into how these algorithms justify specific parameter recommendations to medical physicists and radiologists.

5. **Limited Personalization Based on Clinical Indication**

   Several studies have explored dose reduction strategies while maintaining diagnostic image quality for specific CT examinations. However, most AI applications do not yet dynamically adjust scanning parameters according to the clinical purpose of the examination, which could further enhance both radiation protection and diagnostic efficiency. This gap has been highlighted in recent scoping reviews [22].

6. **Lack of Integration of Cumulative Radiation Exposure**

   Current AI models for dose optimization primarily focus on predicting or reducing radiation exposure for individual CT examinations. The cumulative radiation exposure history of patients is rarely incorporated into existing decision-support systems, even though long-term radiation risk is known to be cumulative in nature [2, 10]. Integrating this information could significantly improve personalized radiation protection strategies in clinical practice.

2.5 Discussion and Positioning of the Proposed Work

An important advancement in CT imaging has occurred with the development of AI-based personalized CT imaging protocols, which constitute a shift from standard CT imaging protocols [22, 18]. The primary challenge of implementing an AI-based dose reduction program in the clinical setting is the need to achieve a balance between patient radiation exposure and diagnostic quality [2]. This section reviews the current state of the art, highlights the limitations of existing methods, and positions the proposed thesis as a new paradigm for risk-informed prospective CT dose optimization.

Synthesis of Findings

The review of current research shows that CT imaging is shifting from standard protocols toward more personalized methods. Studies by Liu et al. [30] and Park et al. [28] have proven that deep learning is effective at reducing image noise, which allows for lower radiation doses without losing diagnostic detail. Similarly, Tamura et al. [27] showed that reconstruction algorithms can maintain the clarity of a scan even when the dose is significantly reduced.

The synthesis indicates that while AI has mastered "noise management," it has yet to achieve "protocol mastery." The balance between patient safety and image quality is currently achieved through back-end processing rather than front-end optimization, leaving a significant gap in the proactive application of the ALARA (As Low As Reasonably Achievable) principle [2, 3].

2.6 Comparison Between Prior Studies and the Proposed Work

The reviewed studies, while demonstrating significant advances in CT dose optimization, differ from the present work in several fundamental dimensions. First, regarding the target population, the majority of prior studies focused exclusively on adult patients. Meineke et al. [25] used 3,199 chest CT examinations from adult cohorts, and Tekin et al. [26] applied their model to 551 adult abdominal scans. In contrast, the present study is specifically designed for pediatric patients ranging from 5 days to 16 years of age, a population with substantially higher radiosensitivity and for whom personalized dose management is clinically more critical. Second, concerning the scope of the task, previous works typically addressed a single objective, either dose prediction or image reconstruction improvement. Tamura et al. [27] and Park et al. [28] focused solely on post-acquisition image quality enhancement through Deep Learning Reconstruction, while Tekin et al. [26] and Meineke et al. [25] limited their contributions to DLP or CTDIvol prediction. The present work, by contrast, integrates three complementary tasks within a unified pipeline: regression for dose prediction, classification for radiation risk stratification, and rule-based protocol recommendation aligned with the ALARA principle. Third, with respect to biological personalization, none of the reviewed studies incorporated patient-specific radiosensitivity factors derived from ICRP recommendations into their modeling framework. The proposed work explicitly encodes age-dependent and sex-dependent sensitivity weights, yielding a biologically grounded risk score that reflects individual vulnerability rather than relying solely on physical dose metrics. Finally, regarding explainability and clinical deployability, most prior studies present their models as offline evaluation tools without a clinical inference interface. The present work includes an interactive decision support interface that generates real-time, patient-specific protocol recommendations, representing a step toward practical clinical integration. In summary, while prior studies have established the feasibility of AI-driven dose optimization, the proposed framework advances the field by addressing pediatric specificity, multi-task integration, biological risk personalization, and prospective protocol recommendation within a single coherent system.

2.7 Conclusion

This chapter concludes that CT dose optimization has evolved from conventional hardware-based methods to deep learning approaches and personalized risk assessment strategies. Despite significant progress, important research gaps remain, including limited data diversity, poor generalizability, the ”black-box” nature of AI models, lack of cumulative radiation history integration, and insufficient personalization based on clinical indication. These gaps form the foundation for the proposed work, which aims to provide more comprehensive, transparent, and patient-centered solutions for prospective CT dose optimization.

3 Methodology and Results

3.1 Introduction

This chapter describes the methodology developed to build an intelligent pipeline for predicting CT radiation dose (CTDIvol and DLP) and assessing patient-specific radiation risk in pediatric patients using machine learning. The dataset is first described in terms of sources, composition, and relevant clinical variables. Preprocessing steps are then detailed, including anatomical feature extraction from DICOM images, fusion with clinical metadata, missing value imputation, and feature engineering guided by ICRP recommendations. The data splitting strategy, feature scaling, and four machine learning models—`Random Forest`, `Gradient Boosting`, `Support Vector Machine`, and `Multi-Layer Perceptron`—are subsequently presented, along with the experimental setup (hardware, hyperparameter tuning, and cross-validation) and SHAP-based model explainability. After establishing the methodology, regression results for CTDIvol and DLP prediction, as well as classification results for risk level prediction, are reported with visual summaries. The chapter concludes with a discussion and critical interpretation of the findings. Unlike prior studies that focused on adult populations or conventional regression, this work emphasizes pediatric-specific risk assessment.

3.2 Dataset Description

Initial Data Exploration

The primary objective of this study was to develop a machine learning model applicable to all age groups (from children to adults) and various anatomical regions, with the goal of achieving a comprehensive dose optimization solution. To this end, we initially proposed the American Association of Medical Physicists' (AAPM) Low-Dose Computed Tomography (LDCT) Grand Challenge dataset [31], but it was not available on their website. We contacted them via email (2026.aapm@aapm.org), and they provided it to us via the link: `https://aapm.app.box.com/s/eaw4jddb53keg1bptavvvd1sf4x3pe9h`. This dataset contains high-quality CT images and comprehensive descriptive data for adult patients [31]. However, considering the need to cover the full range of age groups (0 to 95 years and older) and multiple anatomical regions (thorax, abdomen, pelvis, etc.), a substantial amount of data would be required. Based on the data volume typically required for multi-patient and multi-region computed tomography (CT) studies, where even a small cohort of adult patients confined to a single anatomical region can demand tens of gigabytes due to the size of the DICOM files, this volume exceeded the computing and storage resources available for this study [32]. Therefore, after careful consideration, the focus was redirected toward a more specialized and age-appropriate pediatric medical

dataset, which would still allow for the development of a robust model within the study's limitations.

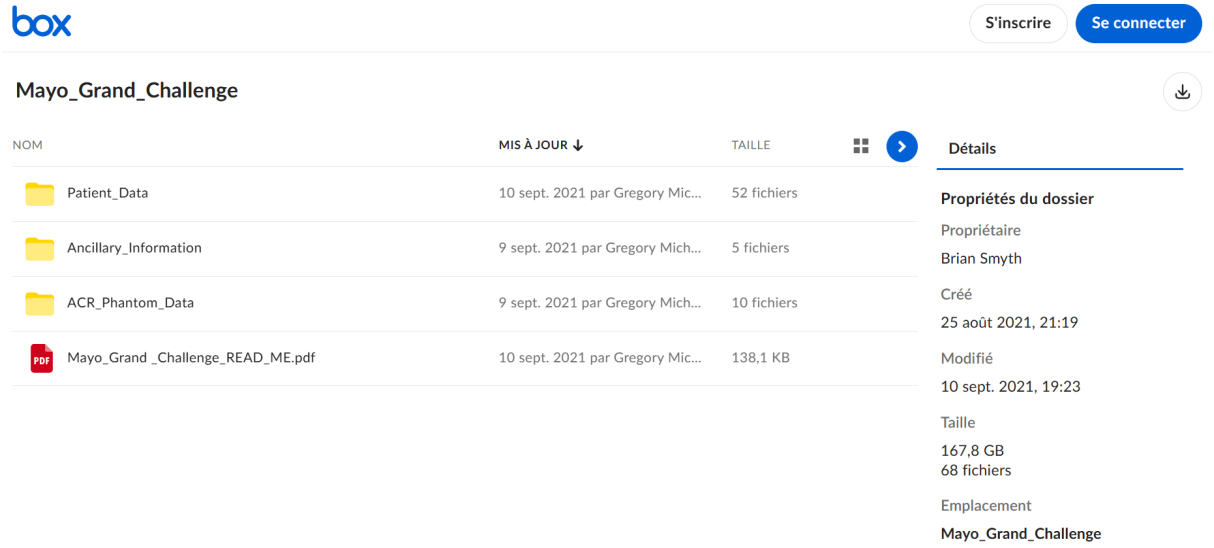

Figure 3.1: *Example from the AAPM LDCT Grand Challenge dataset*

Pediatric-CT-SEG Dataset Characteristics

Based on the limitations identified with the AAPM dataset, we selected the **Pediatric-CT-SEG** collection from The Cancer Imaging Archive (TCIA) [33].This dataset comprises CT examinations from 359 pediatric patients (180 male, 179 female) ranging in age from 5 days to 16 years (mean age 7 years), covering the full range of pediatric age groups: neonates and infants (0–1 year), young children (2–5 years), school-age children (6–10 years), and adolescents (11–16 years). Both male and female patients were included, with approximately balanced sex distribution. The collection contains DICOM CT images acquired from two different CT scanners (GE and Siemens). The total imaging size is approximately 61 GB, and the metadata includes patient age, sex, and weight when available. This dataset is specifically designed for patient organ dose estimation, making it particularly suitable for our pediatric CT dose optimization objective [33].

Final Dataset Composition

After downloading the Pediatric-CT-SEG dataset [33], we performed the following steps to construct our final master table for model training.

Image Processing: Using the `pydicom` library in Python, we processed the DICOM CT scans to extract anatomical features not readily available in the metadata.

Data Integration: The image-derived features were then merged with the clinical metadata (age, sex, weight, scanner settings) using the unique patient identifier, creating a unified tabular dataset.

Handling Missing Values: Missing values were addressed using distinct strategies for each feature:

- **Weight:** Missing weight values were estimated using age-based pediatric growth charts from the World Health Organization (WHO) [34].

- **Tube Voltage (kVp):** This parameter was extracted directly from the DICOM headers of each examination [35].
- **Tube Current-Time Product (mAs):** The mAs value was not directly available in the metadata. According to the DICOM Standard PS3.3, the `Exposure` tag (0018,1152) is defined as *"the product of exposure time and X-Ray Tube Current expressed in mAs"* [36]. Therefore, we calculated mAs using the following relationship:

$$mAs = \text{Tube Current (mA)} \times \text{Exposure Time (s)} \tag{3.1}$$

  The tube current (in mA) was extracted from DICOM tag (0018,1151) and the exposure time (in milliseconds) from DICOM tag (0018,1150), which was then converted to seconds [36].
- **Volume CT Dose Index (CTDIvol):** For examinations with missing CTDIvol, we recalculated it using an empirical formula derived from the acquisition parameters:

$$CTDI_{vol} = 40 \times \left(\frac{kVp}{100}\right)^2 \times \left(\frac{mAs}{100}\right) \tag{3.2}$$

  This formula provides an estimate of the volume-weighted CT dose index based on the tube voltage and tube current-time product, normalized to reference values of 100 kVp and 100 mAs. The constant (40) represents a scaling factor appropriate for the scanner models and acquisition protocols used in this study [37, 38].
- **Dose Length Product (DLP):** DLP was then calculated according to the standard definition from the AAPM Report [39]:

$$DLP = CTDI_{vol} \times \text{Scan Length (cm)} \tag{3.3}$$

  where the scan length was extracted from the DICOM metadata representing the total irradiated length along the patient's longitudinal axis [40]. This approach follows the widely accepted methodology for DLP calculation in pediatric CT dose studies [41, 42].

After applying these imputation and recalculation procedures, a complete dataset with no missing values for the primary dosimetric and morphological features was obtained, enabling subsequent machine learning analysis.

Table 3.1: *Sample of the final preprocessed dataset (first 5 rows)*

Age (years)	Weight (kg)	Diameter (mm)	kVp	mAs	CTDIvol (mGy)	DLP (mGy · cm)
10	30.20	144	100	168.56	39.31	1627.43
3	12.01	112	100	57.50	14.55	526.71
15	76.60	228	100	324.00	45.11	3193.79
12	36.10	155	100	116.80	25.96	1455.38
1	9.46	107	100	41.20	11.11	356.21

Scanner Equipment

Examinations were performed on two CT scanner models representing distinct generations of detector technology and dose modulation capabilities:

- **GE Revolution CT**: a wide-detector, high-speed scanner with 256-slice acquisition capability and ASiR-V iterative reconstruction. Key technical specifications include a gantry rotation time of 0.28 s and tube voltage options of 80, 100, 120, and 140 kVp [43].
- **Siemens SOMATOM Definition AS+**: a dual-source scanner with CARE Dose4D tube current modulation and SAFIRE iterative reconstruction. The system features automatic tube current adjustment based on patient attenuation and real-time anatomy detection [44].

The heterogeneity of scanner models was intentionally preserved in the dataset to improve the generalizability of the trained models and to reflect realistic multi-center clinical conditions [45]. Scanner manufacturer and model were encoded as numerical features (one-hot encoding) in the machine learning pipeline.

3.3 Machine Learning Methodology

Feature Engineering

Raw clinical variables were supplemented by a set of engineered features designed to capture physiologically meaningful interactions and to encode domain knowledge from medical physics:

- **Age radiosensitivity factor (age_sens):** a stepwise function derived from ICRP Publication 103 recommendations, assigning higher weighting to younger patients ($\times 3.0$ for age $\leq$ 1 year, $\times 2.5$ for 2–5 years, $\times 2.0$ for 6–10 years, $\times 1.5$ for 11–16 years) [2].
- **Sex radiosensitivity modifier (sex_factor):** female patients were assigned a factor of 1.15 relative to male patients (1.0), reflecting higher gonadal and breast tissue sensitivity to ionizing radiation [2].
- **Combined radiosensitivity score (radiosens_score):** calculated as radiosens_score = age_sens $\times$ sex_factor, representing a composite individual vulnerability index.
- **Morphological interaction terms:** two product terms were created:
  - age_x_diam = Age $\times$ Diameter
  - weight_x_scan = Weight $\times$ Scan Length

  These terms model dose dependence on body habitus and examination extent.

- **Body cross-sectional area (body_area_cm^2):** approximated as:

$$\text{body\_area\_cm}^2 = \pi \times \left(\frac{\text{Diameter}}{20}\right)^2 \tag{3.4}$$

  where diameter is in mm. This feature is relevant to X-ray beam attenuation modeling.

- **Binary kVp flag (kvp_bin):** distinguishes high-dose acquisition (kVp $\geq$ 100) from low-dose acquisition (kVp $<$ 100):

$$\text{kvp\_bin} = \begin{cases} 1 & \text{if } kVp \geq 100 \\ 0 & \text{if } kVp < 100 \end{cases} \tag{3.5}$$

- **Age group encoding:** a four-level ordinal variable (0–3) capturing developmental stage:
  - 0: Neonates and infants (0–1 year)
  - 1: Young children (2–5 years)
  - 2: School-age children (6–10 years)
  - 3: Adolescents (11–16 years)

- **Scanner model binary flags:** GE Revolution CT and Siemens SOMATOM Definition AS+ were encoded separately as dummy variables (one-hot encoding).

After feature construction, the final input matrix **X** comprised **19 features** per patient (12 original variables + 7 engineered features).

Table 3.2: *Summary of all features in the final input matrix (19 features)*

Feature Name	**Type**	**Origin**
Age (years)	Continuous	Original
Sex (M/F)	Categorical	Original
Weight (kg)	Continuous	Original
Body diameter (mm)	Continuous	Original
kVp	Discrete	Original
mAs	Continuous	Original
Scan length (cm)	Continuous	Original
Slice thickness (mm)	Discrete	Original
Manufacturer (GE/Siemens)	Categorical	Original
age_sens	Continuous	Engineered
sex_factor	Continuous	Engineered
radiosens_score	Continuous	Engineered
age_x_diam	Continuous	Engineered
weight_x_scan	Continuous	Engineered
body_area_cm^2	Continuous	Engineered
kvp_bin	Binary (0/1)	Engineered
age_group	Ordinal (0-3)	Engineered
GE_flag	Binary (0/1)	Engineered
Siemens_flag	Binary (0/1)	Engineered

3.3.1 Radiation Risk Label Generation

A composite risk score was computed as:

$$\text{Risk Score} = \text{DLP} \times \text{age\_sens} \times \text{sex\_factor} \tag{3.6}$$

This formulation integrates the physical dose delivered (DLP) with the individual biological sensitivity of the patient. The resulting distribution of risk scores was then thresholded at the 33rd and 66th percentiles to generate three balanced risk classes:

- **Low risk:** Risk Score $< P_{33}$ (bottom 33% of the distribution)
- **Medium risk:** $P_{33} \leq$ Risk Score $\leq P_{66}$ (middle 33% of the distribution)
- **High risk:** Risk Score $> P_{66}$ (top 33% of the distribution)

This ICRP-consistent, data-adaptive labeling strategy avoids reliance on arbitrary fixed thresholds and ensures approximately equal class representation (33% per class), which is important for balanced classifier training.

Figure 3.2: *Overview of dataset characteristics for the pediatric cohort: (a) age distribution, (b) sex distribution, (c) CTDIvol distribution, (d) DLP distribution, (e) CTDIvol vs. Age by risk level, (f) DLP vs. Weight by risk level, (g) feature correlation matrix, (h) risk label distribution, and (i) CTDIvol by age group.*

3.3.2 Data Splitting and Preprocessing

The dataset was partitioned into a training set (80%, n = 287) and a test set (20%, n = 72) using stratified sampling based on pediatric age groups. Stratification was applied to ensure proportional representation of all four developmental stages in both subsets, preserving the statistical characteristics of the full cohort.

Feature scaling was applied exclusively for the SVM and MLP algorithms, both of which are sensitive to feature magnitude differences. A `RobustScaler` was used rather than the standard `MinMaxScaler` or `StandardScaler`. The `RobustScaler` removes the median and scales the data according to the interquartile range (IQR), making it more resistant to outliers compared to other scaling methods. This is a clinically important property given that pediatric dose data can include extreme values associated with very small infants or obese adolescents. Tree-based models (RF, GB) received the unscaled feature matrix, as they are invariant to monotonic transformations of the input features.

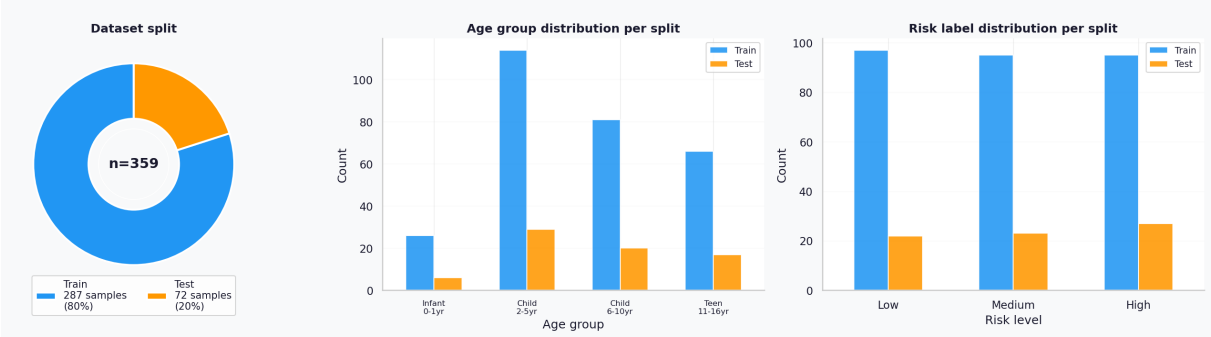

Figure 3.3: *Train-test split performed on age groups: distribution of Infant and Child samples in our experiment*

3.3.3 Model Architectures

Four supervised learning algorithms were implemented and trained for both the regression and classification tasks:

Random Forest (RF)

An ensemble of 300 decision trees, each trained on a bootstrapped sample with random feature subspace selection at each split. Key hyperparameters: `max_depth=12`, `min_samples_split=4`, `min_samples_leaf=2`. The ensemble averages predictions across all trees for regression and uses majority voting for classification.

Gradient Boosting (GB)

An additive boosting ensemble of 300 shallow trees (`max_depth=5`), trained sequentially to minimize the residual error of the previous stage. Key hyperparameters: `learning_rate=0.05`, `subsample=0.8` (stochastic gradient boosting). The reduced learning rate and subsample ratio together serve as regularization mechanisms.

Support Vector Machine / Regression (SVM/SVR)

An RBF-kernel SVM with $C = 100$ for regression ($\epsilon = 0.1$) and $C = 10$ for classification. The high regularization parameter reflects the moderate dataset size and the relatively smooth dose-feature relationship expected from physical principles.

Multi-Layer Perceptron (MLP)

A feed-forward neural network with three hidden layers of 128, 64, and 32 neurons respectively, using ReLU activation, the Adam optimizer, and a learning rate of 0.001. Early stopping (patience=25 iterations without validation loss improvement) was implemented to prevent overfitting, with 10% of the training data held as an internal validation set.

3.3.4 Evaluation Metrics and Cross-Validation Protocol

Model evaluation was performed on the held-out test set using the following metrics:

- **Regression**: Mean Absolute Error (MAE), Root Mean Squared Error (RMSE), and Coefficient of Determination (R^2).
- **Classification**: Accuracy, Precision (macro-averaged), Recall (macro-averaged), and F1-score (macro-averaged), supplemented by per-class confusion matrices and full classification reports.

Additionally, 5-fold cross-validation on the training set was performed for all models to assess variance in performance and detect potential overfitting. Permutation-based feature importance analysis was conducted post-training to identify the most influential predictors.

Table 3.3: *Summary of input features and target variables used in the ML pipeline.*

Variable	Type	Range / Categories	Role in Model
Age (years)	Continuous	0 – 16	Input feature
Sex	Categorical	M / F	Input feature
Weight (kg)	Continuous	3 – 80	Input feature
Body diameter (mm)	Continuous	124 – 245	Input feature
kVp	Discrete	80 / 100 / 120	Input feature
mAs	Continuous	20 – 450	Input feature
Scan length (cm)	Continuous	8 – 45	Input feature
Slice thickness (mm)	Discrete	1.0 / 2.0 / 3.0	Input feature
Manufacturer	Categorical	GE / Siemens	Input feature
CTDIvol (mGy)	Continuous	–	Regression target A
DLP (mGy · cm)	Continuous	–	Regression target B
Radiation Risk	Ordinal	Low / Medium / High	Classification target

3.4 Implementation Framework

In this section we describe the technical environment in which our system was built and executed, including the programming language, development tools and libraries used throughout the implementation.

Hardware Configuration

To implement our system, we used a combination of computing environments. Initially, the dataset was downloaded and preliminary code development was carried out using a university computer. Subsequently, we used a personal laptop for further development and testing. Table 3.4 summarizes the specifications of the personal laptop, while the university computer provided similar or higher computational capabilities with access to institutional storage and networking resources.

Table 3.4: *Personal laptop hardware specifications (HP EliteBook 840 G5)*

Component	Specification
Personal Computer	HP EliteBook 840 G5
Processor	Intel(R) Core(TM) i7-7600U @ 2.80 GHz (up to 2.90 GHz)
RAM	16.00 GB
Hard Drive	238 GB SSD
Graphics	Intel UHD Graphics 620 (128 MB)
Operating System	Windows 11 Pro (21H2)

3.5 Development Language and Tools

This section outlines the programming language and tools used to implement and evaluate the proposed CT dose optimization and radiation risk assessment system.

Python

Python is a high-level, object-oriented, interpreted programming language with dynamic semantics, first released in 1991. It is extremely attractive for rapid application development and for use as a scripting or glue language to join pre-existing components because of its high-level built-in data structures, dynamic typing, and dynamic binding. Python's easy-to-learn syntax prioritizes readability, which lowers software maintenance costs [46]. Python's strengths for machine learning are its readability, simplicity, and abundance of libraries. With frameworks like scikit-learn, TensorFlow, and PyTorch, Python makes it simple to implement complex machine learning algorithms, and its rich ecosystem of data manipulation and visualization tools (like Pandas and NumPy) speeds up model development and experimentation. Additionally, Python has a robust community that ensures ongoing innovation and resources for addressing a variety of machine learning problems [46].

Anaconda

Anaconda is a complete platform for data science and statistical analysis that includes Python along with a number of libraries and tools for data analysis, MLOps, model management, and software development, including Jupyter Notebook, which requires no prior setup. This is the reason we chose to use Anaconda on both the university computer and the personal laptop [47].

Figure 3.4: *Anaconda Logo*

PyTorch

PyTorch is an open-source deep learning framework created by Meta AI. It offers a versatile and efficient platform for creating and training neural networks with the help of dynamic computation graphs and powerful GPU acceleration. PyTorch's performance and ease of use have contributed to its adoption in both academia and industry [48]. In this study, PyTorch was used to implement the Multi-Layer Perceptron (MLP) model.

PIL and Pillow

PIL (Python Imaging Library) is the original Python library for opening, modifying, and storing a wide variety of image file formats [49]. Pillow is a modern fork of PIL, providing extensive support for image processing operations such as loading, manipulating, and saving images in various formats [50]. It is compatible with Python and integrates easily with popular libraries like NumPy and PyTorch [50]. These libraries were used to extract anatomical features from DICOM images during preprocessing.

NumPy

NumPy is an open-source project that makes it possible to use Python for numerical computation. It was developed in 2005, expanding upon the earlier work of the Numeric and Numarray libraries. By consensus of the NumPy and larger scientific Python community, NumPy is developed publicly on GitHub [51]. In this work, NumPy was used extensively for array operations and mathematical computations (e.g., dose formulas).

Scikit-learn (sklearn)

One of the most useful machine learning packages in Python is the scikit-learn library, which offers a variety of powerful methods for statistical modeling and machine learning [52]. Regression, classification, clustering, and dimensionality reduction are some of these

methods [52]. In this study, scikit-learn was used to implement Random Forest, Gradient Boosting, and Support Vector Machine models, as well as for data splitting, feature scaling (RobustScaler), and evaluation metrics (MAE, RMSE, R2, accuracy, precision, recall, F1-score).

Pydicom

Pydicom is a pure Python package for parsing DICOM files [53]. It allows easy extraction of metadata and pixel data from medical imaging files [53]. This library was essential for processing the Pediatric-CT-SEG dataset and extracting parameters such as tube voltage (kVp), tube current (mA), exposure time, scan length, and body diameter from the DICOM headers [54].

Matplotlib and Seaborn

Matplotlib and Seaborn are Python libraries for data visualization [55][56]. They were used in this work to plot training curves (loss vs. epochs), feature importance graphs, dose distribution histograms, and comparison charts between predicted and actual dose values.

OS, Glob, and Shutil

The built-in Python libraries os, glob, and shutil were employed to navigate the directory structure of the Pediatric-CT-SEG dataset [54], to recursively search for DICOM files, and to organize preprocessed image files into structured folders.

TQDM

TQDM (TaQuiD Mi) is a Python library that generates progress bars for loops and long-running operations [57]. It was utilized in this study to monitor feature extraction from thousands of DICOM slices and to track training epochs in an interactive manner.

3.6 Results and Discussion

3.6.1 Regression Task: CTDIvol and DLP Prediction

Performance Metrics Overview

To evaluate model accuracy in predicting the two primary dose metrics (CTDIvol and DLP), several statistical measures were employed: the coefficient of determination (R^2), mean absolute error (MAE), and root mean square error (RMSE). Table 3.5 summarizes the performance of the four models (Random Forest, Gradient Boosting, SVM, MLP) on the test set.

The Gradient Boosting model has an advantage over all other models as it yields better results such as R^2 value of the CTDIvol being 0.9825, R^2 value of the DLP being 0.9424 along with the least amount of error metrics regarding MAE and RMSE in the predictions of DLP. The SVM model was able to predict well for CTDIvol with R^2 of 0.9804 and MAE being 0.873 mGy but did not successfully learn from the complexity of the relationship with DLP, indicating that the SVM model can be very sensitive to the

Table 3.5: *Performance metrics of the four models for CTDIvol and DLP prediction*

Algorithm	CTDIvol (mGy)			DLP (mGy · cm)		
	R^2	MAE	RMSE	R^2	MAE	RMSE
Random Forest	0.9662	1.692	2.973	0.9029	140.4	226.8
Gradient Boosting	0.9825	1.176	2.139	0.9424	106.6	174.6
SVM	0.9804	0.873	2.263	0.6545	261.3	427.6
MLP	0.9556	1.204	3.411	0.9399	125.1	178.4

distribution and nature of the sample data set. The high level of accuracy associated with the Gradient Boosting and Random Forest algorithms is due to their ability to learn and account for the non-linear relationships and interactions between all variables (i.e., weight, age, kVp and mAs), which is reflective of how these factors are known to affect radiation dose in computed tomography.

Actual vs. Predicted Plots

The scatter plots (Figures 3.5 and 3.7) illustrate the relationship between the actual and predicted values for each model. Points clustered around the ideal fit line ($y = x$) reflect model accuracy. The SVM model shows less scatter for lower CTDIvol values, while the MLP model tends to vary for higher values. For DLP, the Gradient Boosting model exhibits the closest convergence, while SVM shows scattered points far from the ideal line, confirming its poor performance in this task. These plots confirm that tree-based and boosting models are the most suitable for this problem.

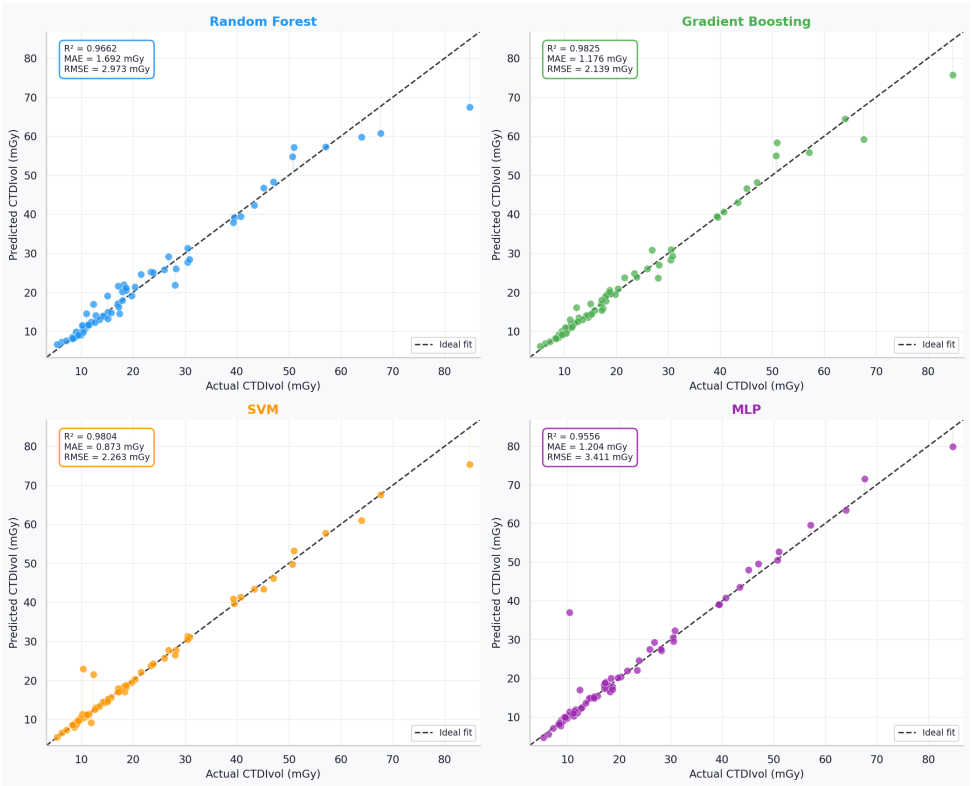

Figure 3.5: *Comparative Performance of Machine Learning Models for CTDIvol Prediction in Pediatric CT Scans*

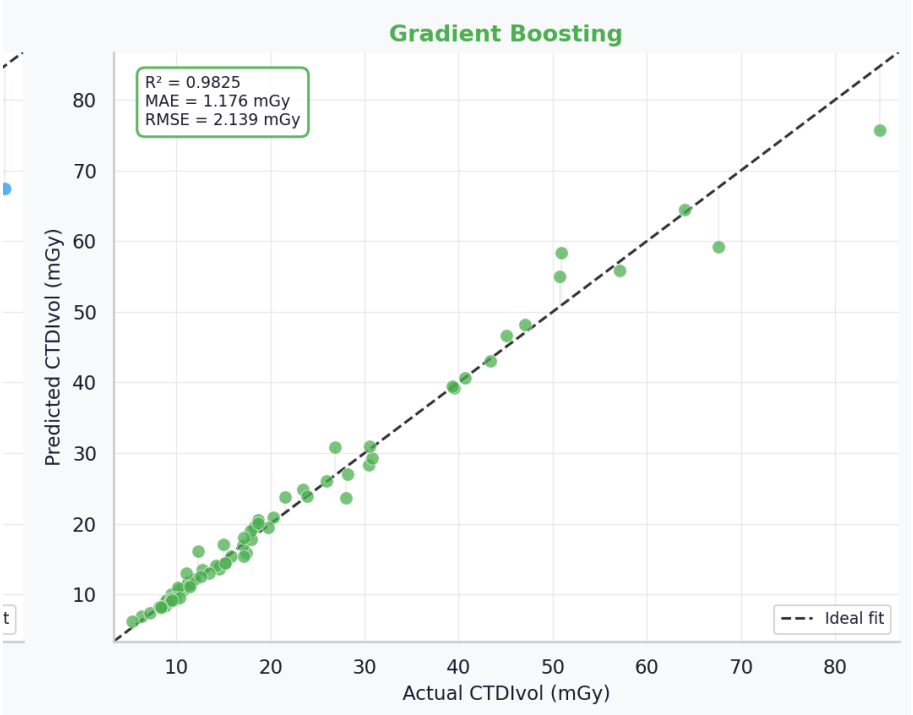

Figure 3.6: *Actual versus Predicted CTDIvol Values for Gradient Boosting Regression Model ($R^2 = 0.9825$)*

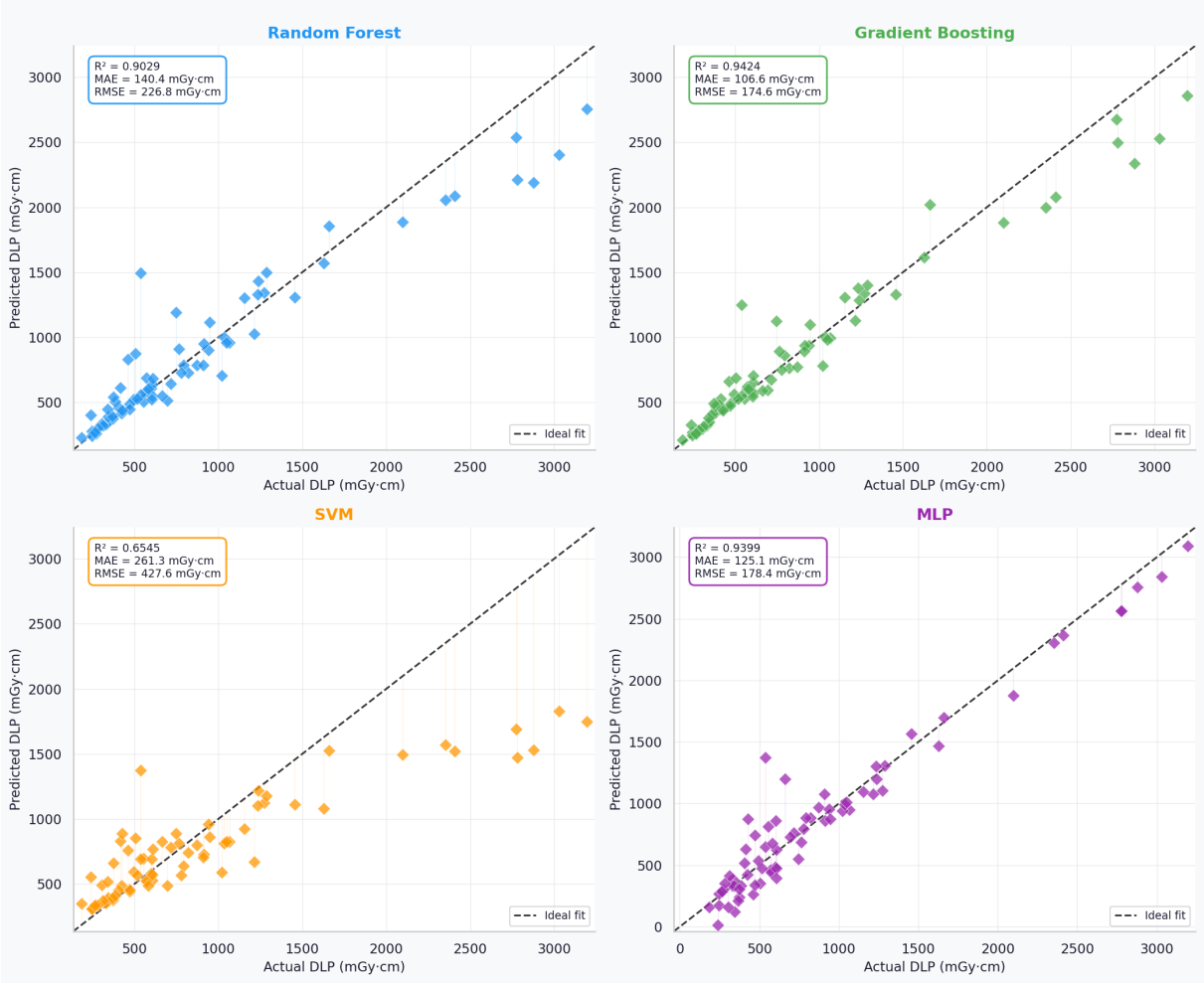

Figure 3.7: *Comparative Performance of Machine Learning Models for DLP Prediction in Pediatric CT Scans*

3.6.2 Classification Task: Radiation Risk Stratification

Risk Label Generation

Patients were stratified into three risk categories (Low, Medium, High) based on a calculated Risk Score defined as (DLP × age-sensitivity factor × sex factor). This method, grounded in International Commission on Radiological Protection (ICRP) recommendations, accounts for variations in radiosensitivity across age groups and sexes, resulting in a relatively balanced distribution of classes (Low: 119, Medium: 118, High: 122 patients), which is essential for effective classifier training.

Classifier Performance Comparison

Table 3.6 summarizes the performance of the four classification algorithms for the risk stratification task.

The MLP model demonstrates a significant advantage across all metrics, surpassing tree-based and traditional machine learning models. The high F1-Score (0.8723) indicates that the model achieves an excellent balance between precision and recall. The SVM model ranks second, while Random Forest shows the lowest performance. This suggests

Table 3.6: *Performance Comparison of Classification Algorithms*

Algorithm	Accuracy	Precision	Recall	F1-Score
Random Forest	0.7222	0.7414	0.7222	0.7268
Gradient Boosting	0.7778	0.7859	0.7778	0.7803
SVM	0.8472	0.8568	0.8472	0.8491
MLP	0.8750	0.8765	0.8750	0.8723

that the nature of the decision boundaries for risk categories may be more complex (potentially non-linear and non-convex) than what tree-based models can capture, while being effectively modeled by the MLP.

Confusion Matrix Interpretation

Figure 3.8 presents confusion matrices for four classifiers (Random Forest, Gradient Boosting, SVM, and MLP) across three risk classes: High, Medium, and Low.

Random Forest shows the weakest performance: it correctly identifies only 19 out of 29 High cases (65.5%), misclassifying 8 as Medium and 2 as Low — both are clinically dangerous errors. It also confuses 4 Low cases as Medium and 1 Low as High.

Gradient Boosting improves High-class accuracy (22/27 correct, 81.5%), with 5 High→Medium errors and no High→Low errors. It also correctly classifies all Medium cases (17/17) without Medium→High errors.

SVM matches Gradient Boosting in High-class performance (22/27 correct, 5 High→Medium errors) but outperforms it in Medium-class accuracy (20/20 correct) and Low-class accuracy (19/22 correct, 86.4%). SVM makes only 1 Low→High error, which is less dangerous than missing a High case.

MLP is the best-performing model from a clinical safety perspective: it correctly classifies 26 out of 27 High cases (96.3%), with only one High→Medium error and no High→Low errors. Low and Medium classes show minimal confusion (1–3 errors each).

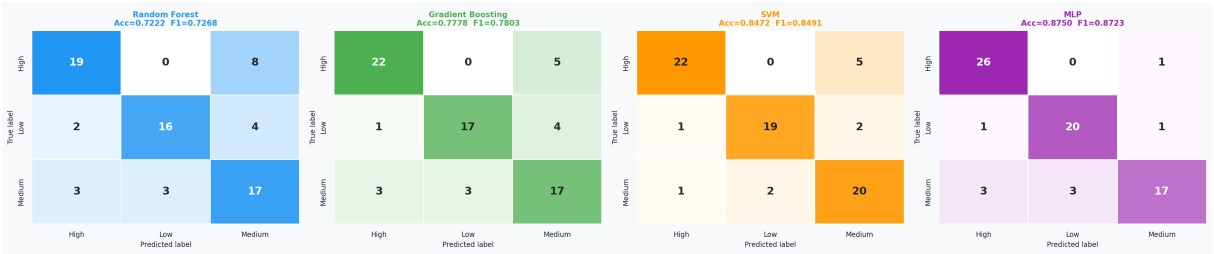

Figure 3.8: *Comparative Confusion Matrices of Machine Learning Models for Personalized Radiation Risk Classification in Pediatric CT*

3.6.3 Protocol Recommendation ALARA Principle

The kVp recommendation logic follows a two-dimensional look-up strategy indexed by age group and predicted risk level, as depicted in the heatmap panel of Figure 3.9. Specifically:

- for infants (0–1 year): 80 kVp is assigned for Low and medium risk and 100 kVp for High risk;

- for young children (2–5 years): 80 kVp is assigned for Low risk, and 100 kVp for Medium and High risk;
- for school-age children (6–10 years): 100 kVp is uniformly applied across all risk levels; and
- for adolescents (11–16 years): 100 kVp is applied for Low and Medium risk, escalating to 120 kVp for High risk to maintain adequate image contrast in larger anatomical cross-sections.

This graduated kVp assignment is grounded in the well-established inverse relationship between tube voltage and photon beam attenuation: lower kVp settings increase photoelectric absorption contrast, benefiting small-diameter patients at the cost of higher skin dose, while higher kVp reduces dose-per-mAs but requires higher current to maintain SNR. The 80 kVp protocol for low-risk infants and young children is consistent with European guidelines (EC Publication No. 185) and published paediatric CT optimisation studies.

The mAs recommendation is derived from an ALARA-adjusted median protocol: the function `clinical_inference()` queries the training dataset for similar patients (within ±2 years of age and ±30% of weight) to extract a reference median mAs. For High-risk patients, a mandatory 15% reduction is applied to this reference value in accordance with iterative reconstruction capability assumptions, yielding the recommended mAs as:

$$\mathrm{mAs}_{\mathrm{rec}} = \begin{cases} 0.85 \times \mathrm{mAs}_{\mathrm{reference}} & \text{(High risk)} \\ \mathrm{mAs}_{\mathrm{reference}} & \text{(Low or Medium risk)} \end{cases} \tag{3.6}$$

This 15% reduction margin was selected to balance dose reduction with the minimum acceptable signal-to-noise ratio threshold for paediatric abdominal CT, as endorsed by the American College of Radiology Dose Index Registry. The central panel of Figure 3.9 superimposes three curves: the actual CTDIvol values sorted by patient index, the Gradient Boosting predicted values, and the ALARA-optimised projection (−15% for High-risk patients). The close tracking between actual and predicted confirms the model fidelity, while the ALARA curve demonstrates a meaningful dose reduction potential: at the highest dose cases (patient indices 60–72), the ALARA-optimised CTDIvol is reduced by 4–15 mGy compared to current practice, representing a clinically significant reduction in stochastic risk for adolescent patients.

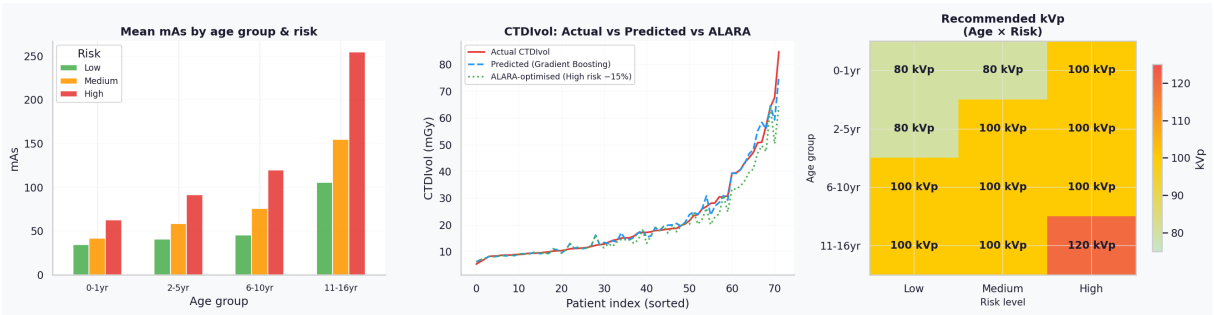

Figure 3.9: *Three-panel visualization of the ALARA-based protocol recommendation system: (left) mean mAs by age group and risk level; (center) comparison of actual CTDIvol, Gradient Boosting predictions, and ALARA- optimized projections (−15group and risk level.*

Clinical Inference Case Studies

An interactive clinical testing interface was implemented using the Gradient Boosting model, identified as the best-performing regressor from earlier comparative analysis (R^2 = 0.9424 for DLP, low MAE/RMSE). The interface allows adjustment of key patient parameters — age, sex, weight, auto-estimated diameter, and scanner type. For a representative test case (9-year-old male, 24 kg, estimated diameter 200 mm, GE scanner), the model predicted a CTDIvol of 10.83 mGy, DLP of 383.0 mGy · cm, and effective dose of 5.75 mSv. The corresponding ALARA-based protocol recommendation (kVp = 100, mAs = 57) was generated automatically. This interactive tool demonstrates the clinical deployability of the Gradient Boosting model, enabling real-time, patient-specific dose predictions with integrated risk assessment (low radiation risk, age sensitivity factor).

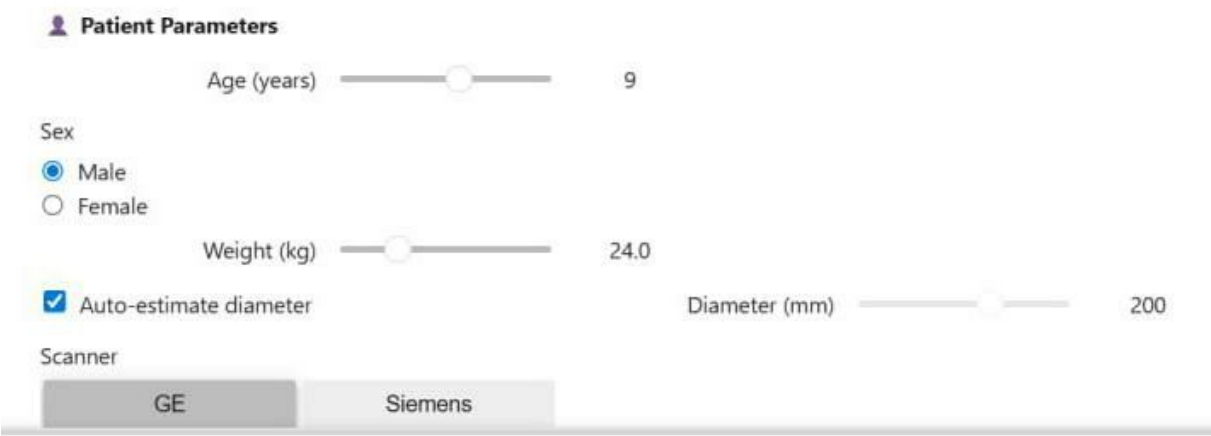

Figure 3.10: *Clinical interface: patient input parameters*

Figure 3.11: *Clinical inference output: dose predictions (CTDIvol, DLP, effective dose) and ALARA-based protocol recommendation*

3.6.4 Limitations

- **Sample Size and Generalizability:** The dataset (n=359) is modest for training neural networks, potentially contributing to the MLP's slightly higher cross-validation variance.
- **Limited Scanner Diversity:** Data from only two scanner manufacturers (GE, Siemens) limits the direct generalizability of the model to other vendors without retraining or adaptation.
- **Surrogate Endpoints:** The study uses dose metrics (CTDIvol, DLP) and a calculated risk score as endpoints, not actual patient outcomes.
- **Missing Image Quality Metric:** The model lacks a noise-to-dose trade-off measure; a truly ALARA-compliant tool requires an integrated measure of image quality.

3.7 Conclusion

This chapter presented a complete methodological framework for predicting CT radiation dose metrics and risk stratification using machine learning. A dataset of **pediatric** CT examinations was processed to extract relevant features, and **four** models were developed and evaluated alongside traditional baselines. The results demonstrated that tree-based and boosting models excelled at regression tasks, capturing the non-linear dose-feature relationships expected from physical principles. For the three-level radiation risk classification task, the MLP achieved the best overall performance. Feature importance analysis revealed that mAs, kVp, and patient diameter were the most influential predictors. The integration of these models into an ALARA-based protocol recommendation system was also explored. While several limitations were identified and discussed, the proposed approach provides a solid foundation for developing a patient-specific clinical decision support system for dose optimization.

General Conclusion

This thesis aimed to develop a machine learning framework for optimizing CT radiation dose and enabling personalized radiation risk assessment in compliance with the ALARA principle. A comprehensive pipeline was established to predict dose metrics (CTDIvol, DLP) and stratify patients into three risk categories (Low, Medium, High) using patient-specific features (age, sex, weight, body diameter, scanner parameters) combined with ICRP-based radiosensitivity factors.

A review of the literature (2015–2025) revealed that most AI approaches focus on post-scan image denoising or isolated dose prediction, with limited integration of cumulative radiation risk or prospective (pre-scan) protocol recommendations. In response, our work proposes a prospective, risk-informed system combining tree-based regressors for dose prediction and a Multi-Layer Perceptron (MLP) for risk stratification.

Experimental results on a pediatric CT dataset of 359 patients demonstrated strong performance. The Gradient Boosting model achieved an R^2 of 0.9825 for CTDIvol and 0.9424 for DLP, while the MLP attained 87.5% accuracy and an F1-score of 0.8723 for risk classification. Feature importance analysis confirmed that mAs, kVp, and patient diameter are the most influential predictors. These findings compare favorably with prior studies by integrating radiosensitivity and prospective protocol logic, thereby addressing a key gap in the literature.

However, several limitations are acknowledged. The dataset size (n=359) is modest, data from only two scanner manufacturers (GE, Siemens) limits generalizability, the study relies on surrogate endpoints (CTDIvol, DLP) rather than actual patient outcomes or image quality metrics, and the absence of a noise-to-dose measure prevents full ALARA compliance.

To address these limitations, the following solutions are proposed:

- **Data expansion** to include more patients (2,000–3,000), multiple centers, and additional scanner vendors (Canon, Philips) through collaborative initiatives like TCIA.
- **Integration of image quality metrics** (SNR, CNR) via multi-task learning to enable explicit dose-quality optimization.
- **Clinical deployment** as a CDS tool integrated into radiology workflow, providing pre-scan kVp/mAs recommendations and risk classification.
- **Cumulative dose tracking** to adjust scan objectives based on lifetime attributable risk (LAR), validated through prospective cohort studies.
- **Integration of explainability methods** (SHAP, LIME) to enhance clinical trust and transparency.

In conclusion, this thesis demonstrates that a machine learning pipeline combining tree-based regressors and a neural network can effectively predict CT dose and personalize radiation risk in a pediatric population. While current limitations related to sample size, scanner diversity, and missing image quality metrics preclude immediate clinical deployment, the proposed framework establishes a solid foundation. By systematically addressing these gaps, the system can evolve into a clinically robust, ALARA-compliant decision support tool that enhances patient safety without compromising diagnostic confidence.

Bibliography

[1] Jerrold T. Bushberg, J. Anthony Seibert, Edwin M. Leidholdt, and John M. Boone. *The Essential Physics of Medical Imaging*. Lippincott Williams & Wilkins, Philadelphia, 3rd edition, 2012.

[2] International Commission on Radiological Protection (ICRP). *The 2007 Recommendations of the International Commission on Radiological Protection*. ICRP Publication 103. Elsevier, Oxford, 2007.

[3] International Atomic Energy Agency (IAEA). *Radiation Protection and Safety of Radiation Sources: International Basic Safety Standards*. IAEA Safety Standards Series No. GSR Part 3. IAEA, Vienna, 2014.

[4] Stewart C. Bushong. *Radiologic Science for Technologists: Physics, Biology, and Protection*. Elsevier, St. Louis, 11th edition, 2017.

[5] Willi A. Kalender. *Computed Tomography: Fundamentals, System Technology, Image Quality, Applications*. Publicis, Erlangen, 2011.

[6] Eric J. Hall and Amato J. Giaccia. *Radiobiology for the Radiologist*. Lippincott Williams & Wilkins, Philadelphia, 8th edition, 2018.

[7] Euclid Seeram. *Computed Tomography: Physical Principles, Clinical Applications, and Quality Control*. Saunders, St. Louis, 4th edition, 2016.

[8] C. Zhang, J. Liu, J. Wu, K. Ranjan, X. Cui, X. Wang, D. Zhang, and S. Zhu. Key molecular dna damage responses of human cells to radiation. *Frontiers in Cell and Developmental Biology*, 12, 2024.

[9] A. Lierova, M. Milanová, J. Pospíchal, J. Novotný, J. Storm, L. Andrejsová, and Z. Sinkorova. Biological effects of low-dose radiation from ct imaging. *Radiation Protection Dosimetry*, 198(9–11):514–520, 2022.

[10] D. Brenner and E. Hall. Computed tomography–an increasing source of radiation exposure. *The New England Journal of Medicine*, 357(22):2277–2284, 2007.

[11] N. Hamada and Y. Fujimichi. Classification of radiation effects for dose limitation purposes: history, current situation and future prospects. *Journal of Radiation Research*, 55:629–640, 2014.

[12] B. Buchberger, K. Scholl, L. Krabbe, L. Spiller, and B. Lux. Radiation exposure by medical x-ray applications. *GMS German Medical Science*, 20, 2022.

[13] Amy Berrington de Gonzalez, Elisa Pasqual, and Lene Veiga. Epidemiological studies of ct scans and cancer risk: the state of the science. *The British Journal of Radiology*, 94(1126):20210471, 10 2021.

[14] World Health Organization. *Communicating Radiation Risks in Paediatric Imaging: Information to Support Healthcare Discussions About Benefit and Risk*, 2016.

[15] World Health Organization and International Atomic Energy Agency. Bonn call for action: 10 actions to improve radiation protection in medicine in the next decade. https://www.who.int/publications/m/item/bonn-call-for-action, 2014. Joint statement by WHO and IAEA, published 12 August 2014.

[16] American Association of Physicists in Medicine. *Size-Specific Dose Estimates (SSDE) in Pediatric and Adult Body CT Examinations*, 2011. Task Group 204.

[17] European Commission. *European Guidelines on Diagnostic Reference Levels for Paediatric Imaging*, 2018.

[18] Cynthia H. McCollough. Milestones in ct: Past, present, and future. *Radiology*, 307(3):e220803, 2023.

[19] Liqiang Ren, Xinhui Duan, Richard Ahn, Fernando Kay, Laleh Daftaribesheli, Wei Zhou, Jeffrey Guild, and Lakshmi Ananthakrishnan. Photon-counting detector ct: technology overview and radiation dose reduction. *British Journal of Radiology*, 98(1175):1788–1801, 2025. Published online: 27 May 2025.

[20] European Radiology Experimental. Photon-counting ct: A disruptive innovation in medical imaging. *European Radiology Experimental*, 9(1):25, 2025.

[21] European Journal of Radiology. Photon-counting ct: An updated review of clinical results. *European Journal of Radiology*, 185:111889, 2025.

[22] M. Bani-Ahmad, A. England, L. McLaughlin, Y. H. Hadi, and M. McEntee. Potential of artificial intelligence for radiation dose reduction in computed tomography: A scoping review. *Radiography*, 31(4):102968, 7 2025. Published online: 7 May 2025.

[23] S. Singh, M. K. Kalra, and S. Do. Deep learning in ct image reconstruction: Techniques and clinical applications. *RadioGraphics*, 42(3):745–761, 2022.

[24] Cynthia H. McCollough, Shuai Leng, Lifeng Yu, Dianna D. Cody, John M. Boone, and Michael F. McNitt-Gray. Ct radiation: Key concepts for gentle and wise use. *RadioGraphics*, 35(6):1706–1721, 2015. Published online: 14 October 2015.

[25] Axel Meineke, Christian Rubbert, Lino M. Sawicki, Christoph Thomas, Yan Klosterkemper, Elisabeth Appel, Julian Caspers, Oliver T. Bethge, Patric Kröpil, Gerald Antoch, and Johannes Boos. Potential of a machine-learning model for dose optimization in ct quality assurance. *European Radiology*, 29(7):3705–3713, 2019.

[26] H. O. Tekin, Faisal Almisned, T. T. Erguzel, Mohamed M. Abuzaid, W. Elshami, Antoaneta Ene, Shams A. M. Issa, and Hesham M. H. Zakaly. Utilization of artificial intelligence approach for prediction of dlp values for abdominal ct scans: A high accuracy estimation for risk assessment. *Frontiers in Public Health*, 10:892789, 2022.

[27] Akio Tamura, Eisuke Mukaida, Yoshitaka Ota, Iku Nakamura, Kazumasa Arakita, and Kunihiro Yoshioka. Deep learning reconstruction allows low-dose imaging while maintaining image quality: comparison of deep learning reconstruction and hybrid iterative reconstruction in contrast-enhanced abdominal ct. *Quantitative Imaging in Medicine and Surgery*, 12(5):2977–2984, 2022.

[28] H. J. Park et al. Deep learning image reconstruction algorithm for abdominal multidetector ct at different tube voltages: assessment of image quality and radiation dose in a phantom study. *European Radiology*, 32:3974–3984, 2022.

[29] B. Moradmand Bahonar, A. Ebrahiminia, V. Changizi, and S. Baradaran. Prediction of breast dose in chest ct examinations using adaptive neuro-fuzzy inference system (anfis). *Physical and Engineering Sciences in Medicine*, 46:1071–1080, 2023.

[30] Xiao-Jing Liu, Yan-Hui Yang, Yue-Hong Guo, Yan-Li Li, and Wei Chen. The application of deep learning-based artificial intelligence algorithms combined with low-dose scanning protocols in chest ct. *Quantitative Imaging in Medicine and Surgery*, 14(5):3250–3262, 2024.

[31] Cynthia H McCollough, Adam C Bartley, Rickey E Carter, Baiyu Chen, Tammy A Drees, Phillip Edwards, David R Holmes III, Alice E Huang, Farhana Khan, Shuai Leng, Kyle L McMillan, Gregory J Michalak, Kristina M Nunez, Lifeng Yu, and Joel G Fletcher. Low-dose ct for the detection and classification of metastatic liver lesions: Results of the 2016 low dose ct grand challenge. *Medical Physics*, 44(10):e339–e352, 2017.

[32] Spie-aapm lung ct challenge. https://www.cancerimagingarchive.net/collection/spie-aapm-lung-ct-challenge/. 70 patients, approximately 12.1 GB.

[33] Petr Jordan, Philip M. Adamson, Vrunda Bhattbhatt, Surabhi Beriwal, Sangyu Shen, Oskar Radermecker, Supratik Bose, Linda S. Strain, Michael Offe, David Fraley, Sara Principi, Dong Hye Ye, Adam S. Wang, John Van Heteren, Nghia-Jack Vo, and Taly Gilat Schmidt. Pediatric chest-abdomen-pelvis and abdomen-pelvis ct images with expert organ contours. *Medical Physics*, 49(5):3523–3528, 5 2022.

[34] World Health Organization. Who child growth standards: Weight-for-age. https://www.who.int/tools/child-growth-standards, 2006.

[35] DICOM Standards Committee. Digital imaging and communications in medicine (dicom) standard ps3.3, 2021.

[36] DICOM Standards Committee. Digital imaging and communications in medicine (dicom) ps3.3: Information object definitions, 2021. Section C.8.7.2, Table C.8-27: Exposure (0018,1152) is defined as the product of exposure time and X-Ray Tube Current expressed in mAs. Available at: https://dicom.nema.org.

[37] R. L. Dixon. *The Physics of CT Dosimetry: CTDI and Beyond*. CRC Press, 2021.

[38] H. W. Goo. Individualized volume ct dose index determined by cross-sectional scanning and anthropomorphic phantom: a retrospective analysis of pediatric chest ct protocols. *Pediatric Radiology*, 41(8):982–988, 2011.

[39] AAPM Task Group 23. The measurement, reporting, and management of radiation dose in ct. Technical Report AAPM Report No. 96, American Association of Physicists in Medicine, 2008.

[40] American College of Radiology. Dose index registry (dir) measures document. https://nrdrsupport.acr.org, 2014.

[41] Priyanka, R. Kadavigere, and S. Sukumar. Estimation of radiation dose and establishment of local diagnostic reference levels for computed tomography of head in pediatric population. *Journal of X-Ray Science and Technology*, 30(5):983–991, 2022.

[42] Yu Peilin, Fan Wenliang, Lei Ziqiao, et al. Size-specific dose estimation for chest ct examination in pediatric and adult patients. *Chinese Journal of Radiological Medicine and Protection*, 39(1):26–30, 2019.

[43] GE Healthcare. *Revolution CT Technical Reference Manual*, 2020.

[44] Siemens Healthineers. Somatom definition as: Technical specifications. https://www.siemens-healthineers.com, 2021.

[45] D. P. Frush, K. J. Strauss, and M. J. Goske. Radiation dose optimization in pediatric ct: Current concepts and future directions. *Radiology*, 299(2):267–280, 2021.

[46] Python Software Foundation. *Python Reference Manual*, 2006. Version 2.4.3, Available at: https://docs.python.org/3/reference/.

[47] Anaconda Inc. *Anaconda Distribution Documentation*, 2024. Available at: https://docs.anaconda.com/anaconda/.

[48] Meta AI. *PyTorch Documentation*, 2024. Available at: https://pytorch.org/docs/stable/.

[49] PythonWare. *Python Imaging Library (PIL)*. Available at: https://python-pillow.org/.

[50] Pillow Contributors. *Pillow Documentation*. Available at: https://pillow.readthedocs.io/.

[51] NumPy Developers. *NumPy Documentation*. Available at: https://numpy.org/doc/stable/.

[52] F. Pedregosa, G. Varoquaux, A. Gramfort, V. Michel, B. Thirion, O. Grisel, M. Blondel, P. Prettenhofer, R. Weiss, V. Dubourg, J. Vanderplas, A. Passos, D. Cournapeau, M. Brucher, M. Perrot, and E. Duchesnay. Scikit-learn: Machine learning in python. *Journal of Machine Learning Research*, 12:2825–2830, 2011.

[53] Pydicom Contributors. *pydicom Documentation*. Available at: https://pydicom.github.io/pydicom/stable/.

[54] Petr Jordan, Philip M. Adamson, Vrunda Bhattbhatt, Surabhi Beriwal, Sangyu Shen, Oskar Radermcker, Supratik Bose, Linda S. Strain, Michael Offe, David Fraley, Sara Principi, Dong Hye Ye, Adam S. Wang, John Van Heteren, Nghia-Jack Vo, and

Taly Gilat Schmidt. Pediatric chest-abdomen-pelvis and abdomen-pelvis CT images with expert organ contours. *Medical Physics*, 49(5):3523–3528, 2022.

[55] J. D. Hunter. Matplotlib: A 2d graphics environment. *Computing in Science & Engineering*, 9(3):90–95, 2007.

[56] M. L. Waskom. Seaborn: Statistical data visualization. *Journal of Open Source Software*, 6(60):3021, 2021.

[57] C. da Costa-Luis, S. K. Larroque, K. Altendorf, H. Mary, R. Sheridan, M. Korobov, H. Yorozu, and S. Lee. *tqdm: A Fast, Extensible Progress Bar for Python and CLI*, 2024. Available at: https://github.com/tqdm/tqdm.

الجمهورية الجزائرية الديمقراطية الشعبية
People's Democratic Republic of Algeria

وزارة التعليم العالي والبحث العلمي
Ministry of Higher Education and Scientific Research

جامعة غرداية
University of Ghardaia

كلية العلوم والتكنولوجيا
Faculty of Science and Technology

قسم الرياضيات والاعلام الآلي
Department of Mathematics and Computer Science

ترخيص بمناقشة مذكرة ماستر
Master Thesis Defense Permission

I, the undersigned, Mr(s). Youcef Mahdjoub .....
Hereby certify that I have examined the work entitled :
. CT Dose Optimization and Personalized Radiation Risk Assessment for Pediatric Patients using AI
Presented to the partial fulfillment of the Master degree in Computer Science by:

1. • Adjila Ami na ...
2. • Bega Ahlam ....

I reviewed the document, and declare it is free from any serious defaults and respects the academic integrity rules. Furthermore, my jury member proposal is the following:

Dr. Slimane Bellaouar	MCA	Univ.Ghardaia	President
M. Abdelfateh Bekkair	MAB	Univ.Ghardaia	Examiner
M. Saad Boudabia	MCA	Univ.Ghardaia	Supervisor
M. Youcef Mahdjoub	MAA	Univ.Ghardaia	Co-Supervisor

Issued for all due intents and purposes.

Ghardaia, on . 10 / 06 / 2026

Signature

الجمهورية الجزائرية الديمقراطية الشعبية
وزارة التعليم العالي والبحث العلمي

جامعة غرداية
كلية العلوم والتكنولوجيا
قسم الرياضيات والاعلام الالي

الرقم:...../ق.ر.ا/ك.ع.ت/ج.غ

شهادة الترخيص بالإيداع

أنا الأستاذ: سليمان بالاعور

المسؤول عن التصحيح مذكرة الماستر الموسومة بـــ

Risk CT Dose Optimization and Personalized Radiation Assessment for Pediatric Patients using AI

من انجاز الطالبة: أحلام بقة

والطالبة: أمينة عجيلة

شعبة: اعلام الي

تخصص: الانظمة الذكية لاستخراج المعارف

تاريخ المناقشة: 2026/06/22

أشهد ان الطالبات قد قمن بالتعديلات والتصحيحات المطلوبة من طرف لجنة المناقشة، وأن المذكرة قد استوفت جميع شروطها وبإمكانهن إيداعها على مستوى مكتبة الكلية.

غرداية في 07 جويلية 2026

امضاء المسؤول عن التصحيح

سليمان بالاعور

رئيس القسم

رئيس قسم الرياضيات والإعلام الآلي
الحاج موسى ياسين

جامعة غرداية
قسم الرياضيات و الاعلام الآلي
كلية العلوم والتكنولوجيا